used after fixation and permeabilization of cells using a Cytofix/Cytoperm Kit (BD Biosciences).

Histology

At 48 hours after the challenge with hapten, the ears of B6 mice were excised and fixed in 10% formaldehyde. Sections of 5-μm thickness were prepared and stained with hematoxylin and eosin.

FITC-induced cutaneous DC migration

The shaved abdomens of the mice were painted with 200 μl of 2% FITC (Sigma-Aldrich) dissolved in a 1:1 (v/v) acetone/dibutyl phthalate (Sigma-Aldrich) mixture, and the iNOS inhibitor was applied through intraperitoneal injection (2.5 mg in 0.5 ml PBS) twice daily for 4 days. Cutaneous DCs migrating into the draining inguinal and axillary lymph nodes were then counted by means of flow cytometry (Kabashima *et al.*, 2007) using Flow-Count Fluorospheres (Beckman Coulter, Fullerton, CA). The principle of Flow-Count Fluorospheres is based on the precise mixing of microparticles whose concentration and volume are known. Before flow cytometric analysis, 10 μl of Flow-Count Fluorospheres were added to each specimen. The percentages of fluorospheres and migrating DCs within each node were then determined using the FACSCanto system (BD Biosciences). To find the number of migrating DCs, the ratio of DCs to fluorospheres was counted using the following formula, based on Reimann *et al.* (2000), with some modifications: number of migrating DCs = (percentage of migrating DCs/percentage of fluorospheres) × number of fluorospheres.

Chemotaxis assay

EC suspensions were incubated for 9 hours with or without the iNOS inhibitor, and then tested for transmigration across uncoated 5-μm transwell filters (Corning Costar, Corning, NY) to CCL21 or medium in the lower chamber for 3 hours. Migrating cells were enumerated by means of flow cytometry (Ngo *et al.*, 1998). The medium used in this assay was RPMI-1640 with 0.5% fatty acid-free bovine serum albumin (Calbiochem, San Diego, CA).

Apoptosis analysis

The EC suspensions from B6 mice were stained with PE-Cy5-conjugated anti-MHC class II mAb for 20 minutes on ice, then stained with FITC-conjugated Annexin V and propidium iodide (BD Pharmingen, Franklin Lakes, NJ), according to the manufacturer's protocol. The number of LCs was assessed by means of flow cytometry with anti-MHC class II and APC-conjugated anti-CD11c mAbs. Apoptosis in LCs was analyzed using a FACSCanto system with FlowJo software.

Statistical analysis

Data were analyzed using an unpaired two-tailed *t*-test. $P<0.05$ was considered to be significant.

CONFLICT OF INTEREST
The authors state no conflict of interest.

ACKNOWLEDGMENTS
This work was supported in part by a Grant-in-Aid for Scientific Research from the Ministry of Education, Culture, Sports, Science, and Technology of Japan, the Ministry of Health, Labor, and Welfare of Japan, and by a Grant from Shiseido Co. Ltd.

SUPPLEMENTARY MATERIAL

Supplementary material is linked to the online version of the paper at http://www.nature.com/jid

REFERENCES

Akiba H, Kehren J, Ducluzeau MT, Krasteva M, Horand F, Kaiserlian D *et al.* (2002) Skin inflammation during contact hypersensitivity is mediated by early recruitment of CD8+ T cytotoxic 1 cells inducing keratinocyte apoptosis. *J Immunol* 168:3079–87

Arany I, Brysk MM, Brysk H, Tyring SK (1996) Regulation of inducible nitric oxide synthase mRNA levels by differentiation and cytokines in human keratinocytes. *Biochem Biophys Res Commun* 220:618–22

Bennett CL, van Rijn E, Jung S, Inaba K, Steinman RM, Kapsenberg ML *et al.* (2005) Inducible ablation of mouse Langerhans cells diminishes but fails to abrogate contact hypersensitivity. *J Cell Biol* 169:569–76

Cals-Grierson MM, Ormerod AD (2004) Nitric oxide function in the skin. *Nitric Oxide* 10:179–93

Cruz MT, Neves BM, Goncalo M, Figueiredo A, Duarte CB, Lopes MC (2007) Effect of skin sensitizers on inducible nitric oxide synthase expression and nitric oxide production in skin dendritic cells: role of different immunosuppressive drugs. *Immunopharmacol Immunotoxicol* 29:225–41

Diefenbach A, Schindler H, Donhauser N, Lorenz E, Laskay T, MacMicking J *et al.* (1998) Type 1 interferon (IFNalpha/beta) and type 2 nitric oxide synthase regulate the innate immune response to a protozoan parasite. *Immunity* 8:77–87

Fukunaga A, Khaskhely NM, Sreevidya CS, Byrne SN, Ullrich SE (2008) Dermal dendritic cells, and not Langerhans cells, play an essential role in inducing an immune response. *J Immunol* 180:3057–64

Kabashima K, Shiraishi N, Sugita K, Mori T, Onoue A, Kobayashi M *et al.* (2007) CXCL12–CXCR4 engagement is required for migration of cutaneous dendritic cells. *Am J Pathol* 171:1249–57

Kaplan DH, Jenison MC, Saeland S, Shlomchik WD, Shlomchik MJ (2005) Epidermal Langerhans cell-deficient mice develop enhanced contact hypersensitivity. *Immunity* 23:611–20

Kissenpfennig A, Henri S, Dubois B, Laplace-Builhe C, Perrin P, Romani N *et al.* (2005) Dynamics and function of Langerhans cells *in vivo*: dermal dendritic cells colonize lymph node areas distinct from slower migrating Langerhans cells. *Immunity* 22:643–54

Kissenpfennig A, Malissen B (2006) Langerhans cells—revisiting the paradigm using genetically engineered mice. *Trends Immunol* 27:132–9

Kuchel JM, Barnetson RS, Halliday GM (2003) Nitric oxide appears to be a mediator of solar-simulated ultraviolet radiation-induced immunosuppression in humans. *J Invest Dermatol* 121:587–93

Lu L, Bonham CA, Chambers FG, Watkins SC, Hoffman RA, Simmons RL *et al.* (1996) Induction of nitric oxide synthase in mouse dendritic cells by IFN-gamma, endotoxin, and interaction with allogeneic T cells: nitric oxide production is associated with dendritic cell apoptosis. *J Immunol* 157:3577–86

Morita H, Hori M, Kitano Y (1996) Modulation of picryl chloride-induced contact hypersensitivity reaction in mice by nitric oxide. *J Invest Dermatol* 107:549–52

Mowbray M, Tan X, Wheatley PS, Rossi AG, Morris RE, Weller RB (2008) Topically applied nitric oxide induces T-lymphocyte infiltration in human skin, but minimal inflammation. *J Invest Dermatol* 128: 352–60

Musoh K, Nakamura N, Ueda Y, Inagaki N, Nagai H (1998) Possible role of nitric oxide in IgE-mediated allergic cutaneous reaction in mice. *Int Arch Allergy Immunol* 115:91–6

Nagao K, Ginhoux F, Leitner WW, Motegi SI, Bennett CL, Clausen BE *et al.* (2009) Murine epidermal Langerhans cells and langerin-expressing dermal dendritic cells are unrelated and exhibit distinct functions. *Proc Natl Acad Sci USA* 106:3312–7

Ngo VN, Tang HL, Cyster JG (1998) Epstein-Barr virus-induced molecule 1 ligand chemokine is expressed by dendritic cells in lymphoid tissues and strongly attracts naive T cells and activated B cells. *J Exp Med* 188:181–91

Ormerod AD, Dwyer CM, Reid A, Copeland P, Thompson WD (1997) Inducible nitric oxide synthase demonstrated in allergic and irritant contact dermatitis. *Acta Derm Venereol* 77:436–40

Qureshi AA, Hosoi J, Xu S, Takashima A, Granstein RD, Lerner EA (1996) Langerhans cells express inducible nitric oxide synthase and produce nitric oxide. *J Invest Dermatol* 107:815–21

Reimann KA, O'Gorman MR, Spritzler J, Wilkening CL, Sabath DE, Helm K *et al.* (2000) Multisite comparison of CD4 and CD8 T-lymphocyte counting by single- versus multiple-platform methodologies: evaluation of Beckman Coulter flow-count fluorospheres and the tetraONE system. The NIAID DAIDS New Technologies Evaluation Group. *Clin Diagn Lab Immunol* 7:344–51

Rocha IM, Guillo LA (2001) Lipopolysaccharide and cytokines induce nitric oxide synthase and produce nitric oxide in cultured normal human melanocytes. *Arch Dermatol Res* 293:245–8

Ross R, Gillitzer C, Kleinz R, Schwing J, Kleinert H, Forstermann U *et al.* (1998) Involvement of NO in contact hypersensitivity. *Int Immunol* 10:61–9

Ross R, Reske-Kunz AB (2001) The role of NO in contact hypersensitivity. *Int Immunopharmacol* 1:1469–78

Saeki H, Moore AM, Brown MJ, Hwang ST (1999) Cutting edge: secondary lymphoid-tissue chemokine (SLC) and CC chemokine receptor 7 (CCR7) participate in the emigration pathway of mature dendritic cells from the skin to regional lymph nodes. *J Immunol* 162:2472–5

Sanchez-Sanchez N, Riol-Blanco L, Rodriguez-Fernandez JL (2006) The multiple personalities of the chemokine receptor CCR7 in dendritic cells. *J Immunol* 176:5153–9

Schuler G, Steinman RM (1985) Murine epidermal Langerhans cells mature into potent immunostimulatory dendritic cells *in vitro*. *J Exp Med* 161:526–46

Stallmeyer B, Kampfer H, Kolb N, Pfeilschifter J, Frank S (1999) The function of nitric oxide in wound repair: inhibition of inducible nitric oxide-synthase severely impairs wound reepithelialization. *J Invest Dermatol* 113:1090–8

Sugita K, Kabashima K, Atarashi K, Shimauchi T, Kobayashi M, Tokura Y (2007) Innate immunity mediated by epidermal keratinocytes promotes acquired immunity involving Langerhans cells and T cells in the skin. *Clin Exp Immunol* 147:176–83

Tokura Y, Yagi J, O'Malley M, Lewis JM, Takigawa M, Edelson RL *et al.* (1994) Superantigenic staphylococcal exotoxins induce T-cell proliferation in the presence of Langerhans cells or class II-bearing keratinocytes and stimulate keratinocytes to produce T-cell-activating cytokines. *J Invest Dermatol* 102:31–8

Wang R, Ghahary A, Shen YJ, Scott PG, Tredget EE (1996) Human dermal fibroblasts produce nitric oxide and express both constitutive and inducible nitric oxide synthase isoforms. *J Invest Dermatol* 106:419–27

Yamaoka J, Kume T, Akaike A, Miyachi Y (2000) Suppressive effect of zinc ion on iNOS expression induced by interferon-gamma or tumor necrosis factor-alpha in murine keratinocytes. *J Dermatol Sci* 23:27–35

Biochemical and Biophysical Research Communications 391 (2010) 486–491

Contents lists available at ScienceDirect

Biochemical and Biophysical Research Communications

journal homepage: www.elsevier.com/locate/ybbrc

Endothelin-2 is upregulated in basal cell carcinoma under control of Hedgehog signaling pathway

Keiji Tanese [a,b], Mariko Fukuma [a], Akira Ishiko [b], Michiie Sakamoto [a,*]

[a] Department of Pathology, School of Medicine, Keio University, Tokyo 160-8582, Japan
[b] Department of Dermatology, School of Medicine, Keio University, Tokyo 160-8582, Japan

ARTICLE INFO

Article history:
Received 10 November 2009
Available online 13 November 2009

Keywords:
Basal cell carcinoma
Endothelin-2
Hedgehog signaling

ABSTRACT

Vasoactive peptide endothelins are a group of small peptides with diverse paracrine/autocrine actions and are reported to be involved in the pathogenesis of many human malignancies. Basal cell carcinoma (BCC) is a common malignant skin tumor that frequently has aberrant activation of the Hedgehog (HH) signaling pathway. We show here that endothelin-2 (ET-2) is overexpressed in BCC under the control of HH signaling. By real-time quantitative RT-PCR analysis, significant expression of ET-2 mRNA was observed in 19 of 20 cases (95%) compared to normal skin. In addition, inhibition of the HH signaling pathway in a mouse BCC cell line downregulated endogenous ET-2, and activation of HH signaling in mouse embryonic fibroblast upregulated endogenous ET-2. Moreover, the 3′ promoter region of ET-2 gene contains the GLI-binding site and a 0.8 kb downstream fragment containing GLI-binding sites activates transcription in a reporter assay. These data indicate that ET-2 is a direct target gene of HH signaling in BCC.

Introduction

Basal cell carcinoma (BCC) is a common malignant tumor arising in the skin. Recent studies have shown that BCC frequently has abnormalities of the Hedgehog (HH) signaling pathway. HH signaling plays a key role in vertebrate development as it is involved in multiple biological processes, such as cell differentiation, proliferation, and growth [1]. Also, several genes overexpressed in BCC have been reported and downstream signaling pathways of HH signaling are currently being investigated [2–7]. In one of those investigations, we performed DNA microarray analysis using BCC and identified that G-protein-coupled receptor GPR49 (GPR49) is specifically overexpressed in BCC and plays a significant role in cell proliferation [2]. However, the function of the genes reported to be overexpressed is still not sufficient to explain the characteristic features of BCC, including interstitial invasion and angiogenesis; therefore, further understanding of the molecules expressed in BCC and their relation in HH signaling is required.

To identify other candidate genes that play a pathogenic role in BCC, we reexamined our results of DNA microarray analysis and focused on the vasoactive peptide coding gene endothelin-2. The endothelin (ET) family is a group of 21 amino acid peptides with diverse paracrine/autocrine actions [8]. The ET family is composed of three vasoactive peptides, ET-1, ET-2 and ET-3. ET-1 and ET-2 have similar structures, differing by only two amino acids, whereas ET-3 differs in structure in six amino acids [9]. ETs are processed from inactive precursor pro-polypeptides by a subgroup of membrane-bound zinc metalloproteases, the ET-converting enzymes. The three ET isoforms bind to two cell surface receptors, which are seven-transmembrane domain G-protein-coupled receptors: ET receptor subtype A (ET_AR), and subtype B (ET_BR) [10]. ET-1 has the highest affinity for ET_AR, followed by ET-2 and ET-3, with all ETs exhibiting equal affinity for ET_BR [11]. The major role of ETs is controlling vascular tone by acting on vascular smooth muscle cells [12], but recent reports suggest that they are also involved in the pathohistology of various human malignancies [8,9]. Here we report that ET-2 is markedly upregulated in almost all cases of BCC under the control of the HH signaling pathway and show evidence that ET-2 is a direct target of HH signaling.

Materials and methods

Samples. Tumor samples were collected from patients at Keio University Hospital and other affiliated hospitals. Tumor and normal skin were snap-frozen after surgical removal and stored at −80 °C until use. The experiment was approved by the ethics committee of Keio University School of Medicine and all samples were taken after written informed consent was obtained from the patients.

* Corresponding author. Address: Department of Pathology, School of Medicine, Keio University, 35 Shinanomachi, Shinjuku-ku, Tokyo 160-8582, Japan. Fax: +81 3 3353 3290.
E-mail address: msakamot@sc.itc.keio.ac.jp (M. Sakamoto).

0006-291X/$ - see front matter © 2009 Elsevier Inc. All rights reserved.
doi:10.1016/j.bbrc.2009.11.085

Quantitative real-time polymerase chain reaction (QRT-PCR). Total RNA was isolated from tissues and cell lines with an RNeasy Mini Kit, including DNAase treatment (Qiagen KK, Tokyo, Japan). cDNA was synthesized with a Prime Script RT reagent kit (Takara, Kyoto, Japan). QRT-PCR analysis was carried out on TaKaRa PCR Thermal Cycler Dice (Takara) using SYBR Premix Ex Taq (Perfect Real Time) (Takara). Primer sequences for QRT-PCR studies are as follows: human GAPDH primers forward 5′-CCAGCCGAGCCACATCGCTC-3′, reversed 5′-ATGAGCCCCAGCCTTCTCCAT-3′; human ET2 primers forward 5′-TTGGACATCATCTGGGTGAA-3′, reverse 5′- GAAATGT CCCTCAGCCTTTG-3′; human GLI1 primers forwards 5′-GAAGACCT CTCCAGCTTGGA-3′, reversed 5′-GGCTGACAGTATAGGCAGAG-3′; human GLI2 primers forwards 5′-TGGCCGCTTCAGATGACA-GATGTTG-3′, reversed 5′-CGTTAGCCGAATGTCAGCCGTGAAG-3′; mouse Gapdhprimers forwards 5′-TGCACCACCAACTGCTTAG-3′, reversed 5′-GGATGCAGGGATGATGTTT-3′; mouse Et2 primers forwards 5′-TTCTGCCATCGAAGACACTG-3′, reversed 5′- TCCTGCAGCT-CATGGTGTTA-3′; and mouse Gli1 primers forwards 5′-CATTCCACA GGACAGCTCAA-3′, reversed 5′-TGGCAGGGCTCTGACTAACT-3′.

Cell culture. The mouse BCC cell line ASZ001 was kindly provided by Dr. Ervin Epstein (Department of Dermatology, University of California, San Francisco, CA) and Dr. Matthew P. Scott (Department of Developmental Biology, Howard Hughes Medical Institute, Stanford University School of Medicine), and was maintained as reported previously [4]. C3H10T1/2 cells, COS-7 cells, were maintained as described elsewhere [13].

Reagents. Cyclopamine (Biomol Int., Philadelphia, PA) was dissolved in 0.19% ethanol and added to ASZ001 culture at a concentration of 2, 5 or 10 μM. As a control, the same amount of 0.19% ethanol was added. Recombinant Mouse Sonic Hedgehog N Terminus (ShhN). (R&D Systems, Oxford, UK) was dissolved in PBS and added to C3H10T1/2 culture at a concentration of 0.5, 1.0, or 2 μM. As a control, the same amount of PBS was added.

Plasmids, transfection and luciferase assay. ET-2 gene reporter plasmids were constructed by PCR using human genomic DNA. Primers used for PCR are listed below. DNA fragments were treated with restriction enzyme Sal I and BamH I, and inserted into PGL-3 promoter vector (Promega, San Luis Obispo, CA).

Table 1
Expression level of ET-2, GLI1 in BCC.*

Case	Pattern	Lesion	ET-2**	GLI1**
1	Nodular	Face	9.95	43.73
2	Nodular	Face	32.36	24.21
3	Nodular	Face	11.88	13.27
4	Nodular	Face	36.53	102.92
5	Nodular	Face	57.08	81.08
6	Superficial	Trunk	3.56	4.00
7	Nodular	Face	71.75	82.72
8	Nodular	Face	31.93	59.42
9	Superficial	Face	50.23	84.68
10	Superficial	Trunk	1.59	1.33
11	Nodular	Face	5.38	7.06
12	Superficial	Trunk	3.99	10.41
13	Superficial	Trunk	30.94	29.80
14	Superficial	Trunk	9.05	19.86
15	Nodular	Face	18.57	66.31
16	Nodular	Face	38.46	63.46
17	Nodular	Face	26.97	70.66
18	Nodular	Face	21.74	32.22
19	Nodular	Face	19.37	33.26
20	Superficial	Trunk	10.10	17.52

* Each gene expression value represents the ratio of mRNA in the tumor to that in normal skin mRNA.

** Pearson correlation coefficient (two-tailed) was calculated pairwise using Statcel2 software for all combinations ($p < 0.01$). A high correlation was seen between the expression levels of *ET-2* and *GLI1* at $r = 0.807$.

Primer sequences constructed for the reporter of ET-2 promoter regions were as follows: ET2 promoter primers forward 5′-GGAT CCTCTGGTTTTTTGTCTTGGCCA-3′, reverse #1 5′-GTCGACTCATA CTGCAGTGGTGACTCAT-3′, reverse #2 5′-GTCGACTCTTCCTATGAC CACCCAC-3′, reverse #3 5′-GTCGACCCTGGCCTCTTTTGAGTCTT-3′.

As a reference reporter, we used phRL-TK (Promega). Mouse *Gli1* expression vector, reporter constructs of HH signaling, 8 × 3′GBS-luc reporter, and 8 × 3′mut GBS-luc reporter were a gift from Dr. Hiroshi Sasaki (Riken, Kobe, Japan) [5]. Transfection was performed against COS-7, C3H10T1/2, and ASZ001 using Fugene6 (Roche Diagnostics) according to the manufacturer's protocol. Luciferase assay was performed using the Dual-Luciferase Reporter Assay System (Promega) according to the manufacturer's protocol.

Statistical analysis. Statistical analysis was performed using Statcel2 software (OMS, Saitama, Japan). Statistically significant differences were determined by Student's *t*-test.

Results

Overexpression of ET-2 in BCC

As previously reported, DNA microarray analysis in our samples also showed *ET-2* expression to be about 8.1-fold higher than

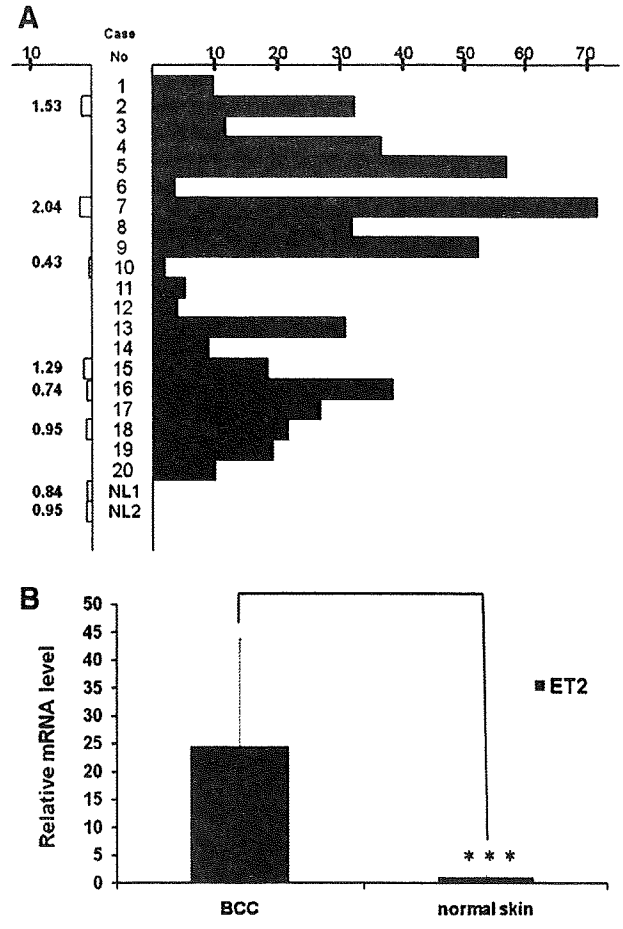

Fig. 1. Overexpression of ET-2 in BCC. (A) QRT-PCR of ET-2. The mRNA levels of ET-2 in 20 BCC and 6 normal skin in the vicinity of BCC, and 2 normal skin samples from non-cancerous patients (NL) are estimated by QRT-PCR (closed column: mRNA level in tumors; open column: mRNA level in normal skin). In normal skin, the expression of ET-2 is negligible compared to BCC. (B) The mean value and SD of each group in QRT-PCR of ET-2. About 24-fold higher levels of ET-2 are shown in BCC in comparison with normal skin.

normal skin [2]. As we could not find or create a specific antibody against ET-2 protein, mainly due to the high similarity with ET-1, we confirmed the expression of *ET-2* by QRT-PCR. Using 20 BCC cases, we analyzed the expression of *ET-2* together with *GLI1*, which were reported to be overexpressed in BCC [3] and to be transcription factors involved in HH signaling (Table 1). Of these 20 cases, 19 showed *ET-2* expression levels more than three times higher than the control (Fig. 1A) (mean increase about 24-fold) (Fig. 1B). On the other hand, the expression by QRT-PCR was low in normal skin samples (Fig. 1A and B).

High relation between ET-2 and HH signaling

Using 20 cases of BCC, the expression of *ET-2* and *GLI1* was confirmed by QRT-PCR, as shown in Table 1. We therefore analyzed the correlation between the expression level of *ET-2* and *GLI1* to evaluate the relation between HH signaling and ET-2. Statistical analysis using Pearson's coefficient was calculated for all combinations. A high correlation was seen between the expression levels of *ET-2* and *GLI1* at $r = 0.807$. HH signaling is activated in BCC, and we speculate here that the expression of *ET-2* is highly related to HH signaling.

To further evaluate the relation between HH signaling and ET-2, we performed an *in vitro* assay using cell lines. Suppression of HH signaling was confirmed by the reporter constructs of HH signaling, 8 × 3′GBS-luc/8 × mut3′GBS-luc [2]. We treated ASZ001 with cyclopamine, a known inhibitor of HH signaling. Downregulation of mouse ET-2 expression was observed together with downregulation of mouse *Gli1*, a target of HH signaling [3], and this downregulation was dependant on the time after treatment and the concentration of cyclopamine (Fig. 2A and B). Next, to see whether ET-2 expression is upregulated by HH signaling, we treated mouse embryonic fibroblast C3H10T1/2 cells, which are known to respond to HH signaling, with ShhN. The expression of mouse ET-2 was increased together with the expression of mouse Gli1 dependant on the time after treatment and the concentration of ShhN (Fig. 3A and B). Upregulation of mouse ET-2 was also confirmed when we transfected mouse Gli1 expression vector [13] to C3H10T1/2 (Fig. 3C). Activation of HH signaling by mouse Gli1 transfection was confirmed by the reporter constructs of HH signaling, 8 × 3′GBS-luc/8 × mut3′GBS-luc (Fig. 3D). These findings indicate that ET-2 is regulated by HH signaling.

Expression of ET-2 is directly regulated by HH signaling

In order to see the direct transcriptional activation of ET-2 by HH signaling, we analyzed a region approximately 1 kb downstream of the ET-2 for motifs identical to or closely matching the GLI-consensus binding site –TGGGTGGTC- [14]. As expected, we found an identical sequence 797–803 b downstream of the ET-2. Thereafter, we constructed three reporter constructs of the ET-2 3′ promoter region, as shown in Fig. 4A. They were transfected to ASZ001, which has endogenous activation of HH signaling. While the reporter plasmid inserted with the ET-2 downstream fragment from 0 to +543 (reporter plasmid #1) showed less reporter activity, significant reporter activity was observed when the reporter plasmid inserted with the downstream fragment from 0 to +815 (reporter plasmid #2) and 0 to 887 (reporter plasmid #3) was transfected to ASZ001 (Fig. 4B).

Next, they were transfected to COS-7 along with a mouse Gli-1 expression vector or an empty vector. The expression of mouse Gli-1 was confirmed by the reporter constructs of HH signaling, 8 × 3′GBS-luc/8 × mut3′GBS-luc [5] (Fig. 4C). Among them, reporter plasmid #2 and reporter plasmid #3 had significant reporter

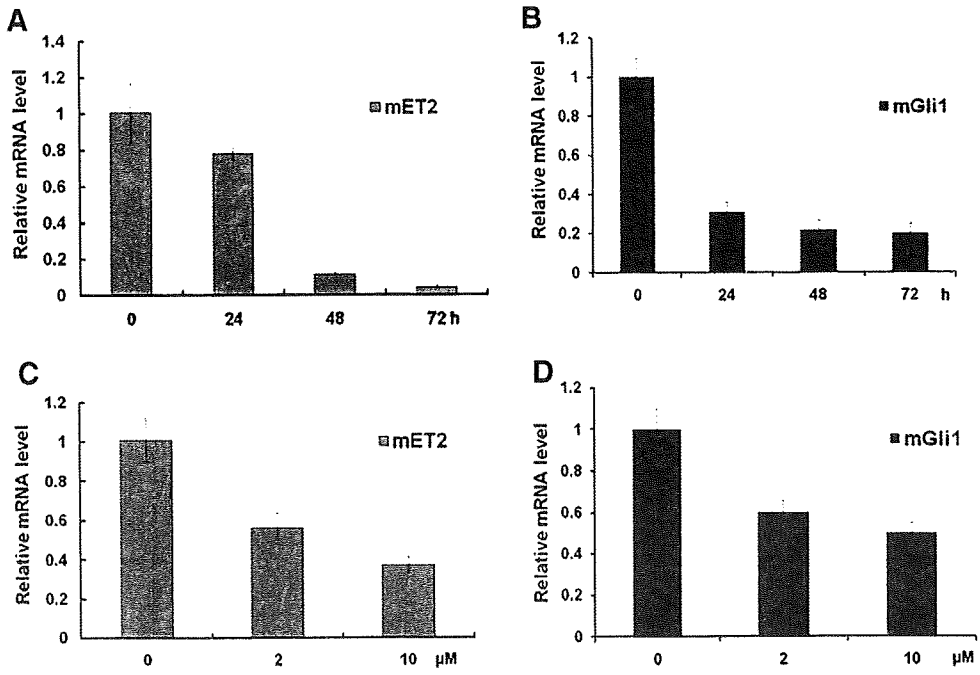

Fig. 2. Suppression of HH signaling decreases ET-2 expression in the mouse BCC cell line ASZ001. (A) Time course of mRNA expression of endogenous mouse ET-2 (m ET-2) and mGli1 in ASZ001 cells treated with cyclopamine. Cells were treated with 10 μM cyclopamine, and expression of m ET-2 (left) and mGli1 (right) mRNA was measured by QRT-PCR at the times shown in the figure. The fold decrease of mRNA levels in cyclopamine-treated to non-treated cells at each sampling time was normalized by setting the baseline value at 1. The figure shows one of the three repeated experiments. Suppression of m ET-2 and mGli1 expression was dependent on the time course. (B) Dose dependency of mRNA expression of m ET-2 and mGli1 on the concentration of cyclopamine. ASZ001 cells were treated with 0, 2, and 10 μM cyclopamine, and expression of m ET-2 (left) and mGli1(right) was measured by QRT-PCR 48 h after treatment. Values are shown as a ratio relative to cyclopamine 0 μM. Suppression of mRNA levels of mET-2 and mGli1 was dependent on the concentration of cyclopamine.

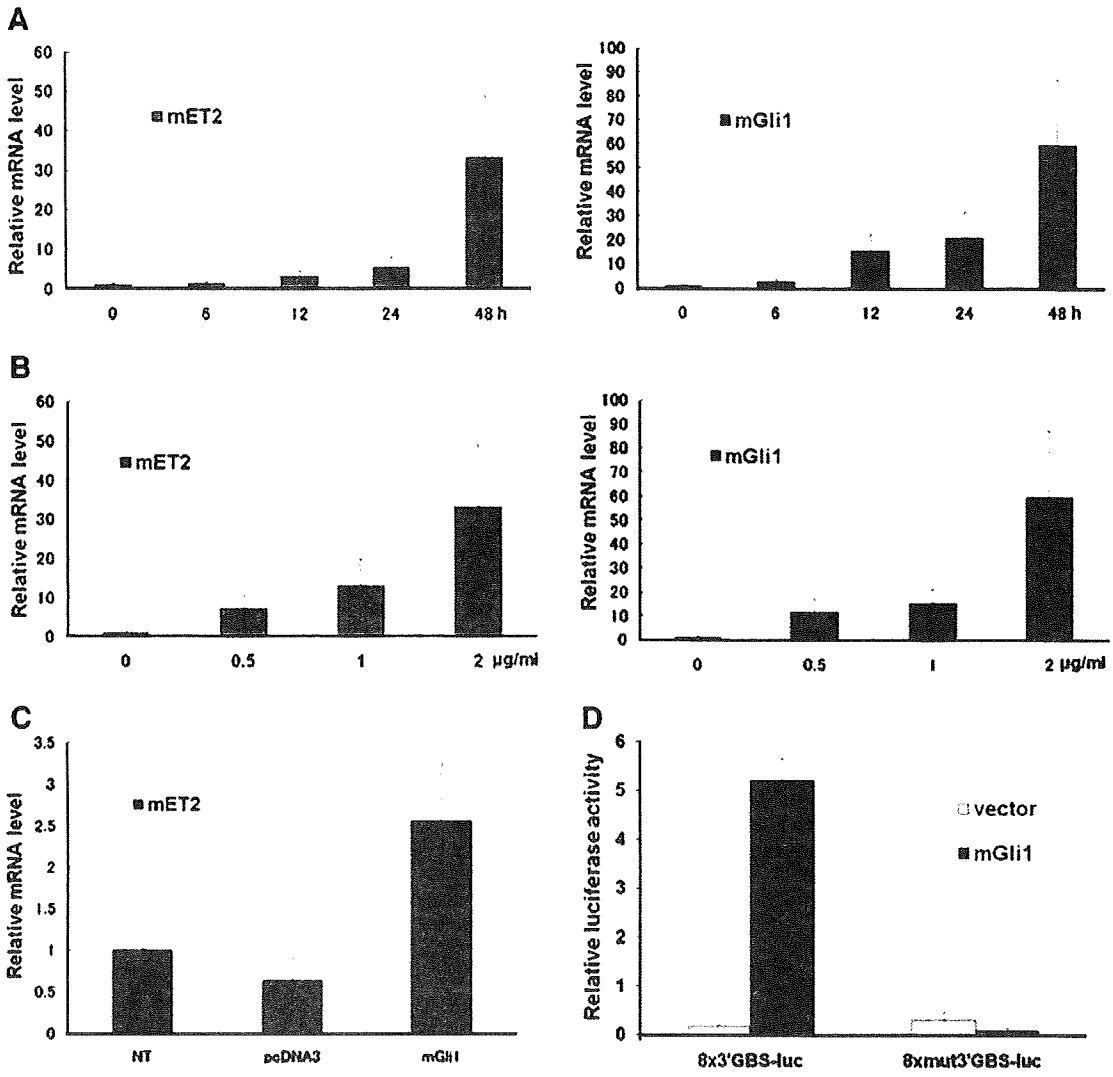

Fig. 3. Activation of HH signaling induces ET-2 expression. (A) Quantitative RT-PCR analysis of endogenous m ET-2 and mGli1 was performed in C3H10T1/2 cells after treatment with ShhN. Cells were treated with 2 μg/ml ShhN for the time indicated in the figure. Upregulation of m ET-2 expression (left) was dependent on the time course, as with mGli1 (right). (B) Dose dependency of mRNA expression of m ET-2 and mGli1 on the concentration of ShhN. C3H10T1/2 cells were treated with 0, 0.5, 1.0 and 2 μg/ml of recombinant N-terminal SHH peptide, and the expression of mET-2 (left) and mGli1 (right) was measured by QRT-PCR 48 h after treatment. Values are shown as a ratio relative to ShhN 0 μg/ml. Expression of mRNA levels of mET-2 and mGli1 was dependent on the concentration of cyclopamine. (C) QRT-PCR analysis of mET-2. Mouse Gli1 expression vector was transfected to C3H10T1/2 cells. mRNA levels of mET-2 were assayed at the time indicated in the figure. The ratios of mRNA level of mGli1-transfected to vector-transfected cells were estimated. When Gli1 is expressed in C3H10T1/2 cells, the gene expression level of mET-2 was elevated. (D) Activation of HH signaling by mGli1-expression vector in C3H10T1/2 cells. Cells were transfected with an mGli1-expression vector, 8 × 3′GBS-luc or 8 × 3′mutGBS-luc, and with phRL-TK as a reference. Luciferase activity was assayed 48 h after transfection. Activity was normalized with those of phRL-TK as a reference. Expression of Gli1 significantly activated the Gli-consensus reporter gene, while a mutant promoter was not affected.

activity when cotransfected with mouse Gli-1 expression vector. On the other hand, reporter activity of the plasmid inserted with fragments from 0 to +543 (reporter plasmid #1) was negligible (Fig. 4D).

Discussion

Our studies showed that ET-2 is overexpressed in BCC. DNA microarray analysis in our samples showed ET-2 expression to be about 8.1-fold higher than normal skin. In QRT-PCR study, ET-2 was markedly overexpressed in 19 of 20 BCC samples of nodular and superficial types in comparison with normal tissue samples. These results suggest that the expression of ET-2 is a characteristic feature in BCC. Expression of ET-2 has not been fully analyzed in the past literature and this is the first report that shows the specific expression of ET-2 in BCC.

Furthermore, our results demonstrated that in BCC, the expression of ET-2 is regulated by the activity of the HH signaling pathway. Our results showed that inhibition of the HH signaling pathway in a mouse BCC cell line downregulated endogenous ET-2, and activation of HH signaling in mouse C3H10T1/2 cells upregulated endogenous ET-2. The presence of a single copy of the GLI-binding site in the putative 3′ promoter region of ET-2, together with the activation of reporter gene expression by this region in the presence of mGli1, points to direct regulation of ET-2 by mGli1. These findings strongly suggest that the expression of ET-2 is regulated by HH signaling directly.

ETs are expressed in a broad range of tumors, and are suggested to play a crucial role in tumor growth, progression, and angiogenesis [15]. Among them, most reports focus on the role of ET-1, which is also reported to be expressed in BCC, and blockade of the ET-1/ETR_A pathway can reduce cell survival *in vitro* [16]. ET-1

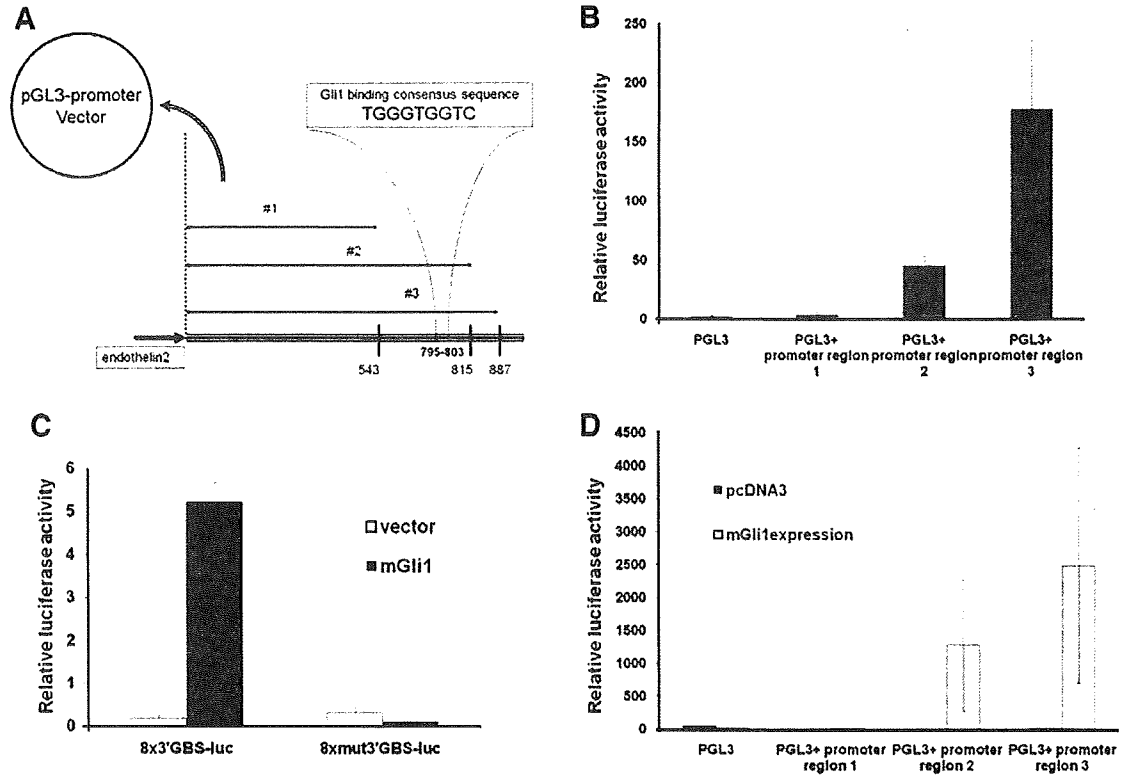

Fig. 4. Analysis of 3′ promoter region of ET-2. (A) The promoter of the human ET-2 gene contains a consensus Gli-binding site. Construction of reporter construct of ET-2 3′ promoter regions. Region between 797 and 803 includes a consensus binding sequence of Gli-1, -TGGGTGGTC-. (B) Reporter activity of ET-2 3′ promoter region in ASZ001. The reporter construct of ET-2 3′ promoter regions was transfected into ASZ001 cells. The relative luciferase activity of the reporter, including the ET-2 downstream fragment from 0 to +815 (reporter plasmid #2) and 0 to 887 (reporter plasmid #3) showed significant luciferase activity. Reporter activity of plasmid inserted with the fragment from 0 to +543 (reporter plasmid #1) was negligible. (C) Reporter activity of HH reporter construct in COS-7. 8 × 3′GBS-luc reporter showed significant reporter activity under the co-transfection of mGli-1 expression vector whereas reporter activity of 8 × 3′mutGBS-luc reporter was negligible. (D) Reporter activity of ET-2 3′ promoter region and HH reporter construct in COS-7. The reporter construct of ET-2 3′ promoter regions and a mouse Gli expression plasmid or empty vector (pcDNA-3) were cotransfected into COS-7 cells. The relative luciferase activity of the reporter including ET-2 downstream fragment from 0 to +815 (reporter plasmid #2) and 0 to 887 (reporter plasmid #3) showed significant luciferase activity when cotransfected with mouse Gli-1 expression vector. Reporter activity of plasmid inserted with fragment from 0 to +543 (reporter plasmid #1) was negligible.

has also been implicated to participate in the pigmentation process of BCC [17]. We also performed QRT-PCR analysis of ET-1 in our BCC samples and confirmed its overexpression (data not shown); however, we could not find a significant relation between ET-1 expression and HH signaling activity. Mouse endogenous ET-1 expression did not change by either inhibiting the HH signaling pathway in ASZ001 cells or activating HH signaling in C3H10T1/2 cells (data not shown). Moreover, we could not find a consensus GLI-binding site in the promoter lesion of human and mouse ET-1; therefore, we speculate that ET-2 rather than ET-1 will play a significant role as a downstream mediator of HH signaling in BCC.

The role of ET-2 in carcinogenesis is still not fully understood. In breast carcinoma, ET-2 is reported to be a hypoxia-induced autocrine survival factor and in invasive ductal carcinoma of the breast, the anti-apoptotic function of ET-2 is reported [18]. With the aim of analyzing the function of ET-2 in BCC, we treated a mouse BCC cell line with BQ-123 (Sigma–Aldrich, St. Louis, MO); a selective ET-RA antagonist, BQ-788 (Sigma–Aldrich); and a selective ET-RB antagonist and ET-2 recombinant protein (Sigma–Aldrich) [19]. However, we could not identify the direct oncogenic role of ET-2 in ASZ001 cells. There was no difference in cell proliferation, cell invasion and cell morbidity between non-treated cells and BQ-123-, BQ-788-, and ET-2-treated cells (data not shown). Therefore, ET-2 may function as a factor affecting the tissues surrounding BCC cells. As one of its putative functions, ET-2 will promote the angiogenesis of BCC. It is known that ETs are angiogenic factors that stimulate the growth of endothelial cells, vascular smooth muscle cells, fibroblast and pericytes in various cancers [20]. BCC also frequently shows a characteristic aberrant angiogenic feature called "arborizing vessels" in dermoscopic findings, which is histopathologically characterized by the proliferation and dilation of dermal capillaries [21]. We speculate that aberrant expression of ET-2 may play some role in this characteristic vascular formation.

Conclusion

We have characterized ET-2 as a novel target gene of the HH signaling pathway in BCC. Functional analysis of ET-2, especially in its role of tumor and interstitial interaction will shed new light on the pathogenesis of BCC.

Conflict of interest

None declared.

Acknowledgments

We thank Dr. Ervin Epstein (Department of Dermatology, University of California San Francisco) and Dr. Matthew P. Scott (Department of Developmental Biology, Howard Hughes Medical Institute, Stanford University School of Medicine) for providing

ASZ001 cells, Dr. Hiroshi Sasaki (Laboratory for Embryonic Induction, RIKEN Center for Developmental Biology) for providing mouse Gli1 expression vector, 8 × 3′GBS-luc reporter and 8 × mutant3′GBS-luc reporter.

This work is support supported by following grants: Grant-in-Aid for the Cancer Research from the Ministry of Education, Culture, Sports, Science and Technology of Japan, The Third Term Comprehensive 10-Year Strategy for Cancer Control from the Ministry of Health, Labor and Welfare of Japan, Research Encouraging Scholarship of Keio University School of Medicine.

References

[1] C. Wicking, E. McGlinn, The role of hedgehog signalling in tumorigenesis, Cancer Lett. 173 (2001) 1–7.
[2] K. Tanese, M. Fukuma, T. Yamada, T. Mori, T. Yoshikawa, W. Watanabe, A. Ishiko, M. Amagai, T. Nishikawa, M. Sakamoto, G-protein-coupled receptor GPR49 is up-regulated in basal cell carcinoma and promotes cell proliferation and tumor formation, Am. J. Pathol. 173 (2008) 835–843.
[3] J.M. Bonifas, S. Pennypacker, P.T. Chuang, A.P. McMahon, M. Williams, A. Rosenthal, F.J. De Sauvage, E.H. Epstein Jr., Activation of expression of hedgehog target genes in basal cell carcinomas, J. Invest. Dermatol. 116 (2001) 739–742.
[4] J. Xie, M. Aszterbaum, X. Zhang, J.M. Bonifas, C. Zachary, E. Epstein, F. McCormick, A role of PDGFRα in basal cell carcinoma proliferation, Proc. Natl. Acad. Sci. USA 98 (2001) 9255–9259.
[5] H. Sasaki, C. Hui, M. Nakafuku, H. Kondoh, A binding site for Gli proteins is essential for HNF-3beta floor plate enhancer activity in transgenics and can respond to Shh in vitro, Development 124 (1997) 1313–1322.
[6] T. Eichberger, G. Regl, M.S. Ikram, G.W. Neill, M.P. Philpott, F. Aberger, A.M. Frischauf, FoxE1, a new transcriptional target of GLI2, is expressed in human epidermis and basal cell carcinoma, J. Invest. Dermatol. 122 (2004) 1180–1187.
[7] C. Cui, T. Elsam, Q. Tian, J.T. Seykora, M. Grachtchouk, A. Dlugosz, H. Tseng, Gli proteins up-regulate the expression of basonuclin in Basal cell carcinoma, Cancer Res. 64 (2004) 5651–5658.
[8] E.R. Levin, Endothelins, N. Engl. J. Med. 333 (1995) 356–363.
[9] T. Masaki, The endothelin family: an overview, J. Cardiovasc. Pharmacol. 35 (2000) S3–5.
[10] B. Haendler, U. Hechler, W.D. Schleuning, Molecular cloning of human endothelin (ET) receptors ETA and ETB, J. Cardiovasc. Pharmacol. 20 (1992) S1–4.
[11] G.M. Rubanyi, M.A. Polokoff, Endothelins: molecular biology, biochemistry, pharmacology, physiology, and pathophysiology, Pharmacol. Rev. 46 (1994) 325–415.
[12] C. Feldstein, C. Romero, Role of endothelins in hypertension, Am. J. Ther. 14 (2007) 147–153.
[13] S. Roman-Roman, D.L. Shi, V. Stiot, E. Haÿ, B. Vayssière, T. Garcia, R. Baron, G. Rawadi, Murine Frizzled-1 behaves as an antagonist of the canonical Wnt/beta-catenin signaling, J. Biol. Chem. 279 (2004) 5725–5733.
[14] K.W. Kinzler, B. Vogelstein, The GLI gene encodes a nuclear protein which binds specific sequences in the human genome, Mol. Cell. Biol. 10 (1990) 634–642.
[15] J. Nelson, A. Bagnato, B. Battistini, P. Nisen, The endothelin axis: emerging role in cancer, Nat. Rev. Cancer. 3 (2003) 110–116.
[16] Y. Zhang, L. Tang, M. Su, D. Eisen, D. Zloty, L. Warshawski, Y. Zhou, Expression of endothelins and their receptors in nonmelanoma skin cancers, J. Cutan. Med. Surg. 10 (2006) 269–276.
[17] C.C. Lan, C.S. Wu, C.M. Cheng, C.L. Yu, G.S. Chen, H.S. Yu, Pigmentation in basal cell carcinoma involves enhanced endothelin-1 expression, Exp. Dermatol. 14 (2005) 528–534.
[18] M.J. Grimshaw, S. Naylor, F.R. Balkwill, Endothelin-2 is a hypoxia-induced autocrine survival factor for breast tumor cells, Mol. Cancer Ther. 1 (2002) 1273–1281.
[19] K. Ishikawa, M. Ihara, K. Noguchi, T. Mase, N. Mino, T. Saeki, T. Fukuroda, T. Fukami, S. Ozaki, T. Nagase, Biochemical and pharmacological profile of a potent and selective endothelin B-receptor antagonist, BQ-788, Proc. Natl. Acad. Sci. USA 91 (1994) 4892–4896.
[20] A. Bagnato, F. Spinella, L. Rosanò, The endothelin axis in cancer: the promise and the challenges of molecularly targeted therapy, Can. J. Physiol. Pharmacol. 86 (2008) 473–484.
[21] G. Argenziano, I. Zalaudek, R. Corona, F. Sera, L. Cicale, G. Petrillo, E. Ruocco, R. Hofmann-Wellenhof, H.P. Soyer, Vascular structures in skin tumors: a dermoscopy study, Arch. Dermatol. 140 (2004) 1485–1489.

Immunoexpression of human epidermal growth factor receptor-2 in apocrine carcinoma arising in naevus sebaceous, case report

Editor

Naevus sebaceous is a hamartoma that combines epidermal, follicular, sebaceous and apocrine gland abnormalities commonly located on the scalp.[1] During adulthood, it has a 10–20% risk of developing into epithelial neoplasms.[2] Among them, most tumours are benign, including syringocystadenoma papilliferum, trichoblastoma, trichilemmoma and sebaceoma.[3] However, several malignant tumours have arisen in this lesion. The most frequently described carcinoma is basal cell carcinoma, but recent studies have confirmed that the vast majority of basaloid neoplasms arising in naevus sebaceous are trichoblastomas and not basal cell carcinoma as once thought.[3] Several types of malignant adnexal neoplasms, including cutaneous apocrine carcinoma (CAC), are also described to occur, but the number of case is limited.[2,4–6]

In this study, we report a 70-year-old Japanese man presented at our clinic with the chief complaint of an enlarging tumour on the scalp. He had a pre-existing hairless plaque since childhood. Two months prior to presentation, a tumour had suddenly aroused on the plaque. Clinical examination of the lesion revealed a reddish dome-shaped nodule, 2 cm in diameter, on a yellowish plaque measuring 3 × 2 cm (fig. 1a). Histological examination of the tumour revealed a moderately differentiated adenocarcinoma infiltrating almost all the thickness of the dermis (fig. 1b). Surrounding skin revealed a typical aspect of naevus sebaceous with epidermal hyperplasia and hyperplastic sebaceous glands. Tumour nests were composed of large glandular lumina and some of them were cystically dilated and contained eosinophilic material resembling apocrine gland lumina (fig. 1c). Lining neoplastic cells of glandular lumina showed decapitation secretion (fig. 1d). The tumour cell had a large nucleus and some mitotic figures were observed. Intracytoplasmic granules were periodic-acid-Schiff (PAS) positive and diastase resistant. Immunohistochemically, these cells showed a positive staining with epithelial membrane antigen (fig. 2a) and gross cystic disease fluid protein-15 (GCDFP-15) (fig. 2b).

On further analysis of the specimen, significant staining of p53 and human epidermal growth factor receptor-2 (HER-2) was observed in the tumour cell (fig. 2c, d). Oestrogen receptor, progesteron receptor and androgen receptor were negative. No other internal malignancy was detected by radiological analysis and we diagnosed this tumour as a CAC arising from naevus sebaceous.

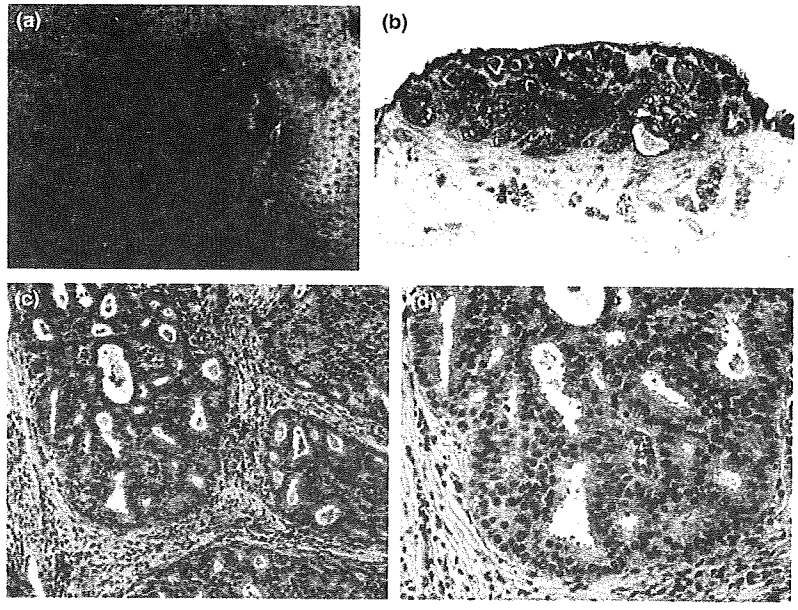

Figure 1 (a) Clinical examination of the lesion revealed reddish dome-shaped nodule, 2 cm in diameter, on a yellowish plaque measuring 3 × 2 cm. Tumour surface was eroded and bled easily. (b) Histological finding. (H.E. macro). Tumour is a moderately differentiated adenocarcinoma infiltrating almost all the thickness of the dermis. (c) Histological finding. (H.E. 100×). Tumour nests were composed of large glandular lumina and some of them were cystically dilated and contained eosinophilic material resembling apocrine gland lumina. (d) Histological finding. (H.E. 200×). Lining neoplastic cells of glandular lumina showed decapitation secretion.

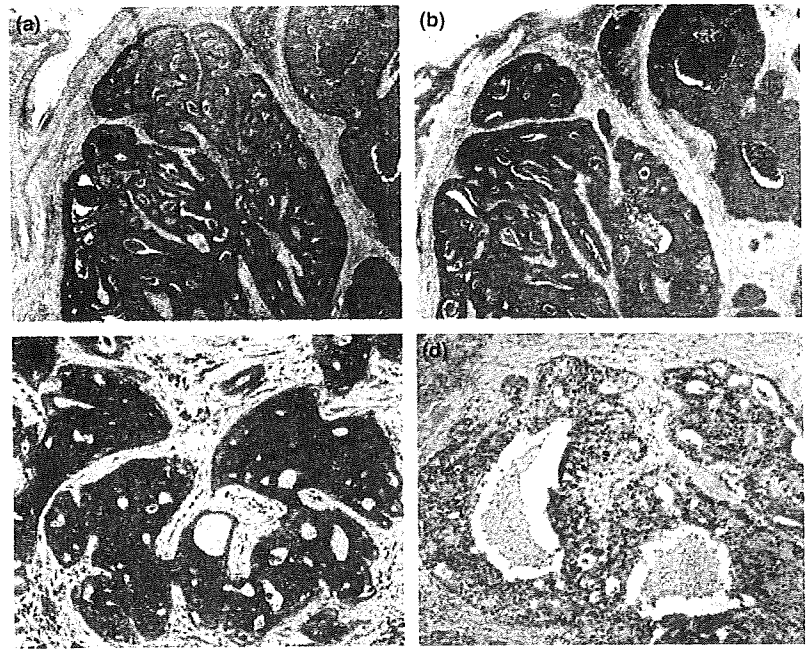

Figure 2 Immunohistochemistry. (a) Expression of epithelial membrane antigen in tumour nest (40×). (b) Expression of gross cystic disease fluid protein-15 in tumour nest (40×). (c) Membranous staining pattern of HER-2 in tumour cells (100×). (d) Nuclear staining pattern of p53 in tumour cells (100×).

Cutaneous apocrine carcinoma is a rare malignancy histologically defined as an adenocarcinoma forming nests of glandular lumina with decapitation secretion of lining neoplastic cells. Tumour cells are PAS-positive, diastase-resistant and positive on immunostaining for GCDFP-15.[7] It develops in areas where apocrine glands are numerous, such as the axilla and the anogenital region. The aetiology of CAC is unknown, but association with naevus sebaceous has been suggested and eight cases are reported.[5,6] As naevus sebaceous develops anomalous dilated apocrine glands in the adulthood, we speculate that some oncogenic events might occur in those hamartomatous apocrine glands, giving rise to CAC. However, molecular event occurring in this tumour is not precisely understood.

Our case showed the immunoexpression of HER-2 and p53 in the tumour cells. HER-2 is a cell membrane surface-bound receptor tyrosine kinase, normally involved in the activation of specific signal transduction pathways including ras/MAP kinase cascade and phosphatidylinositol 3-kinase, leading to cell proliferation and differentiation.[8] Immunoexpression of p53 is known to correlate closely with point mutation of the tumour suppressor gene p53.[9] To our knowledge, there is no report referring to the expression of HER-2 in CAC, whereas it is frequently analysed in breast cancer or extramammary Paget's disease [8,10] that shows pathological features similar to that of CAC. We speculate that overexpression of HER-2 and dysfunctional mutation of p53 might play a crucial role in the development of CAC in our case. Further accumulation of cases and analysis of HER-2 expression in apocrine carcinoma are desired to identify the pathogenesis of this rare tumour.

K Tanese,[†,‡,*] A Wakabayashi,[†,‡] T Suzuki,[‡] S Miyakawa,[†,‡]

[†]Department of Dermatology, School of Medicine, Keio University, Shinjuku-ku, Tokyo, Japan

[‡]Department of Dermatology, Kawasaki Municipal Hospital, Kawasaki, Kanagawa, Japan

*Correspondence: K Tanese. E-mail: tanese@2001.jukuin.keio.ac.jp

References

1 Jadassohn J. II Bemerkungen zur Histologie der systematisierten Naevi und ueber Talgduesen-Naevi. *Arch Dermatol Syph* 1895; 33: 355–394.
2 Domingo J, Helwig E. Malignant neoplasms associated with naevus sebaceous of Jadassohn. *J Am Acad Dermatol* 1979; 1: 454–456.
3 Yoon DH, Jang IG, Kim TY *et al.* Syringocystadenoma papilliferum, basal cell carcinoma and trichilemmoma arising from nevus sebaceous of Jadassohn. *Acta Derm Venereol* 1997; 77: 242–243.
4 Rinaggio J, McGuff HS, Otto R *et al.* Postauricular sebaceous carcinoma arising in association with nevus sebaceus. *Head Neck* 2002; 24: 212–216.
5 Dalle S, Skowron F, Balme B *et al.* Apocrine carcinoma developed in nevus sebaceus of Jadassohn. *Eur J Dermatol* 2003; 13: 487–489.
6 Robson A, Lazar AJ, Ben Nagi J *et al.* Primary cutaneous apocrine carcinoma: a clinico-pathologic analysis of 24 cases. *Am J Surg Pathol* 2008; 32: 682–960.

7 Paties C, Taccagni GL, Papotti M. Apocrine carcinoma of the skin: a clinicopathologic, immunocytochemical, and ultrastructural study. *Cancer* 1993; 71: 375–381.
8 David R, Dennis S. HER-2/neu signal transduction in human breast and ovarian cancer. *Stem Cells* 1997; 15: 1–8.
9 Megha T, Ferrari F, Benvenuto A *et al.* p53 Mutation in breast cancer. Correlation with cell kinetics and cell of origin. *J Clin Pathol* 2002; 55: 461–466.
10 Plaza JA, Torres-Cabala C, Ivan D *et al.* HER-2/neu expression in extramammary Paget disease: a clinicopathologic and immunohistochemistry study of 47 cases with and without underlying malignancy. *J Cutan Pathol* 2009; 36: 729–733.

DOI: 10.1111/j.1468-3083.2009.03407.x

Familiar occurrence of multiple primary epidermoid cysts and trichostasis spinulosa: a novel skin phenotype associated with inherited sensorineural deafness

Editor

A 22-year-old woman presented with a 10-year history of multiple, painful, inflammatory skin lesions, eruptive trichostasis spinulosa (TS) and deafness since early childhood. Loss of hearing started at the age of 6. Skin lesions first occurred after menarche (11.5 years old) and aggravated during the last 5 years. There was a history of inflamed skin lesions and deafness on the paternal side in three consecutive generations: her grandfather, father and four father's cousins.

Clinical examination revealed numerous skin-coloured cysts and inflamed noduli over her neck, back, flexor side of extremities and buttocks, groin and armpits (Fig. 1). Moreover, multiple, dark, spiny follicular papules were distributed over neck, abdomen and buttocks. Follicular ostia were filled up with dark material while hair was prominating from centre. Otorhinolaryngological-audiological examination showed severe bilateral hearing impairment in the high frequencies. Other family members had also moderate to severe hearing impairments since early childhood.

The biopsy of the cyst was performed. Histopathological examination revealed an epidermoid cyst (EC) filled up with keratin (Fig. 2). The diagnosis of TS was made by microscopic examination of hair plug obtained with comedo extractor.

Many different treatment modalities have been tried without benefit, including prolonged courses of different antibiotics, hormonal and isotretinoin therapy with only slight and temporary improvement. At the time she presented to our department, she was given peroral therapy with prednisone to avoid further inflammation. After that, multiple excisions of the cysts were performed for their location and size.

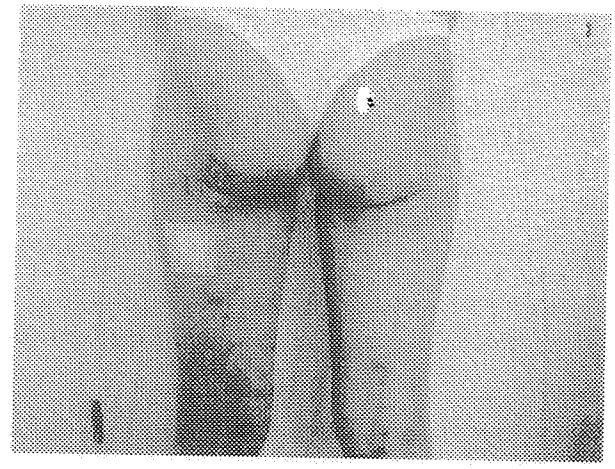

Figure 1 Multiple inflamed and uninflamed noduli and spiny follicular papules over flexor side of extremities and buttocks.

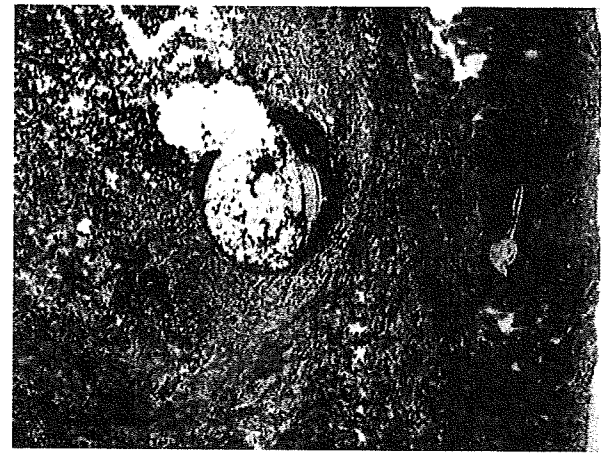

Figure 2 Histopathological finding in skin biopsy revealed an epidermal cyst filled up with keratin; H&E stain, ×20 magnification.

In healthy person, EC are remarkably common, but are usually single or few. Patients with certain hereditary syndromes and patients taking cyclosporine may have multiple primary lesions.[1,2] Regarding TS, because of their characteristic appearance on the face, particularly the nose, some authors consider them to be a variant of the comedonal acne.[3] However, in our patient TS was localized on the neck, chest wall and buttocks in close proximity to EC, with dissemination on abdominal wall.

According to our opinion, this coexistence of two types of lesions on the same skin areas in our patient is likely to reflect the

Correspondence

Extraocular sebaceous carcinoma expressing oestrogen receptor α and human epidermal growth factor receptor 2

doi: 10.1111/j.1365-2230.2009.03654.x

Sebaceous carcinoma (SC) is a rare malignant neoplasm originating in the holocrine adnexal epithelium of sebaceous glands. It can be grossly divided into ocular and extraocular types.

We report a 71-year-old Japanese woman who presented with a 2-year history of an enlarging mass on her right cheek.

On physical examination, a painless, reddish-yellow, dome-shaped mass, measuring 20 mm in diameter was seen on the cheek (Fig. 1a). An excisional biopsy was taken, and an asymmetrical, relatively circumscribed tumour was seen on histopathological examination, consisting of basaloid cells with nuclear atypia and vacuolated cells with sebaceous differentiation (Figs 1b,c). In the surrounding stroma, prominent solar elastosis was seen. The vacuolated cytoplasm was positive for androgen receptor, epithelial membrane antigen and human milk fat globules-1 (Figs 2a,b). The nucleus of the tumour cells was positive for p53 and the labelling index of Ki67 was 15.

The tumour was diagnosed as a moderately differentiated extraocular sebaceous carcinoma. Immunohistochemical staining using anti-oestrogen receptor α (ERα) antibody (Dako, Glostrup, Denmark) and antihuman epidermal growth factor receptor 2 (HER2) antibody (Novocastra, Berlin, Germany) gave strong reactions in most of the tumour cells (Figs 2c,d).

The pathogenesis of SC is still not fully understood. X-ray irradiation and human papillomavirus infection have been reported as tumorigenic factors in ocular SC.[1] However, neither of these applied to our patient (data not shown). In extraocular SC, life-long exposure to ultraviolet radiation (UVR) has been suggested as a tumorigenic factor.[2] The presence of prominent solar

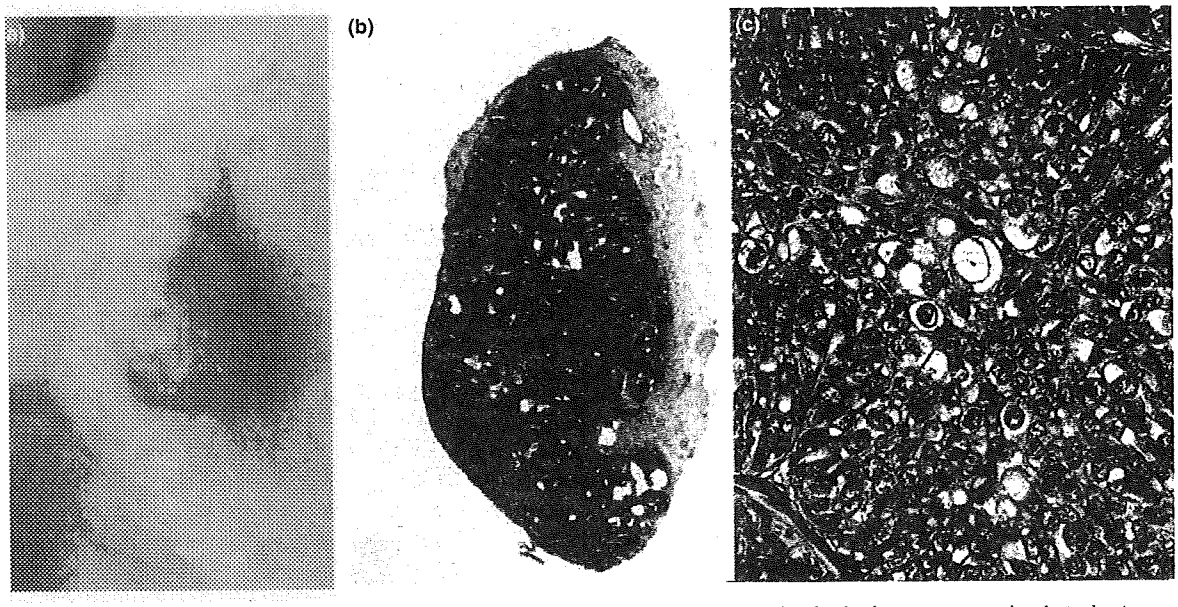

Figure 1 (a) Painless, reddish-yellow, dome-shaped mass of 20 mm in diameter on the right cheek. (b) Asymmetrical, relatively circumscribed tumour consisting of lobules of varying sizes, involving the dermis and subcutaneous tissue. (c) Two types of neoplasm cells: basaloid cells with nuclei atypia and mitotic figures and foamy, vacuolated cytoplasm with sebaceous differentiation. Haematoxylin and eosin, original magnification (a) × 10; (b) × 200.

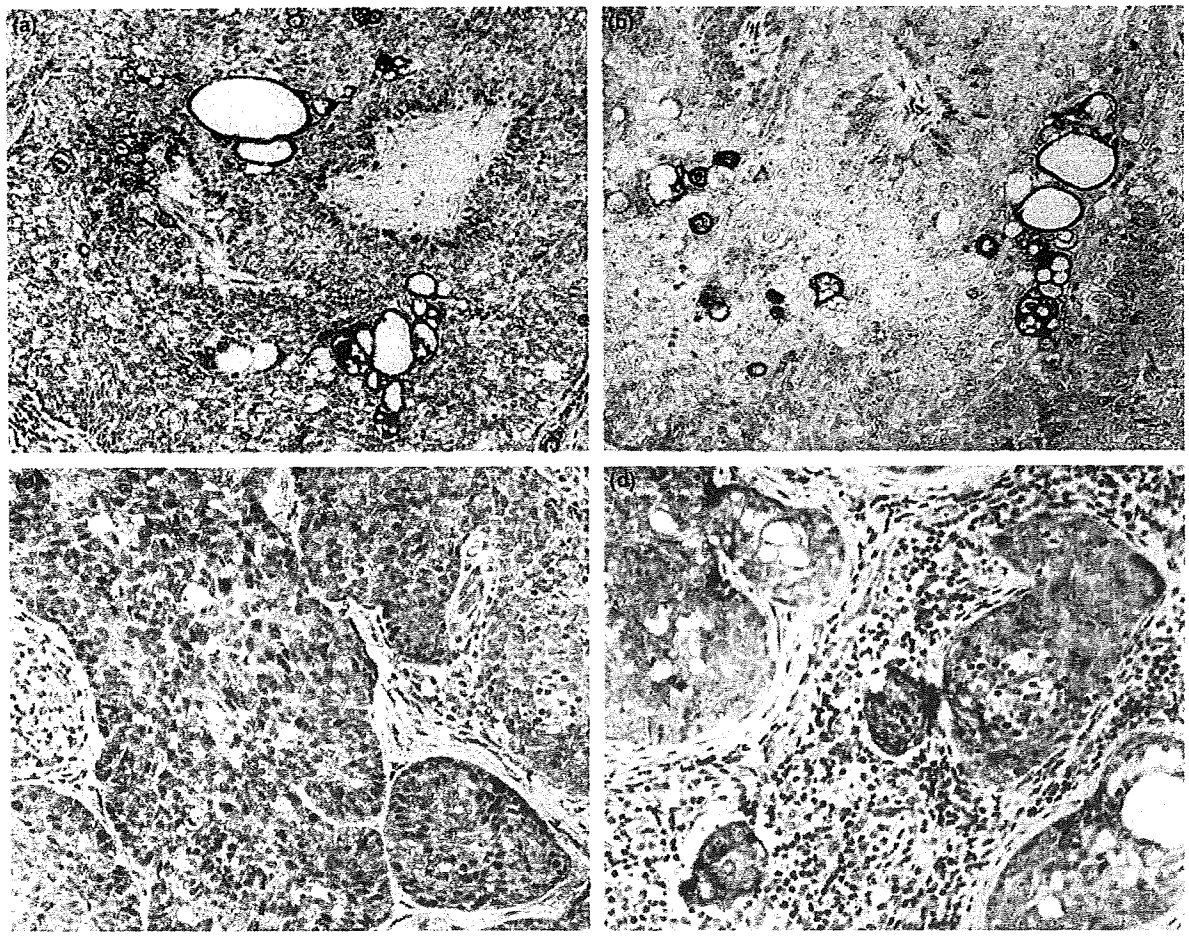

Figure 2 Immunohistochemical staining with (a) epithelial membrane antigen (b) human milk fat globules-1 and (c) oestrogen receptor α and (d) antihuman epidermal growth factor receptor 2. (a, b) Strong expression was seen in vacuolated cytoplasm. (c) Most of the tumour cells stained strongly, and there was also nuclear translocation of ERα. (d) Strong staining of HER2 was seen in the tumour cells, with a membranous staining pattern. The scoring of HER2 immunostaining was 2+. Original magnification (a–d) × 100.

elastosis in our case may suggest UVR as a pathogenic factor.

ERα and HER2 are often expressed in breast cancer and recognized as significant pathogenic factors or targets of treatment. ERα is a member of the nuclear hormone receptor family and considered to cause tumorigenesis by disrupting the cell cycle, apoptosis and DNA repair. HER2 is a cell membrane surface-bound receptor tyrosine kinase, involved in the activation of specific signal-transduction pathways.[3] Whether SC expresses HER2 is controversial, mainly due to the differences in the antibodies and detection methods used in previous studies. One report could not detect the expression of HER2 in seven of eight cases of SC,[4] but another report suggested that expression of HER2 is a marker of poor prognosis in SC.[3] The strong membranous staining in our patient's biopsy supports the role of HER2 expression. The pathogenic role of ERα in SC is still not fully understood. Its expression has been suggested in four cases of ocular SC,[4] and it is reported to be expressed in about 20% of basal cells of sebaceous lobules and 33.3% of benign sebaceous gland neoplasms.[5] However, to our knowledge, no studies have reported expression of ERα in extraocular SC. Because the staining pattern of ERα in our case indicated considerable nuclear translocation, we speculate that some extraocular SCs may also express ERα, and that the receptor may play an important role in cell proliferation.

In conclusion, the expression of these molecules in SC is likely to be important in its pathogenesis. With the accumulation of more cases, perhaps the pathogenesis and treatments can be determined.

A. Wakabayashi,*† K. Tanese,*† K. Yamamoto,† H. Tanomogi† and S. Miyakawa*†
**Department of Dermatology, School of Medicine, Keio University, 35 Shinanomachi, Shinjuku-ku, Tokyo, Japan; and †Department of Dermatology, Kawasaki Municipal Hospital, Shinkawadori, Kawasaki-ku, Kawasaki, Kanagawa, Japan*
E-mail: akiko_wakabayashi@nifmail.jp
Conflict of interest: none declared.
Accepted for publication 21 May 2009

References

1 Gonzalez-Fernandez F, Kaltreider SA, Patnaik BD *et al.* Sebaceous carcinoma Tumor progression through mutational inactivation of p53. *Ophthalmology* 1998; **105**: 497–506.
2 Ansai S, Mihara I. Sebaceous carcinoma arising on actinic keratosis. *Eur J Dermatol* 2000; **10**: 385–8.
3 Hasebe T, Mukai K, Yamaguchi N *et al.* Prognostic value of immunohistochemical staining for proliferating cell nuclear antigen, p53, and c-erbB-2 in sebaceous gland carcinoma and sweat gland carcinoma: comparison with histopathological parameter. *Mod Pathol* 1994; **7**: 37–43.
4 Erik S, Cabral BA, Auerbach A *et al.* Distinction of benign sebaceous proliferations from sebaceous carcinomas by immunohistochemistry. *Am J Dermatopathol* 2006; **6**: 465–71.
5 Kariya Y, Morita T, Suzuki T *et al.* Sex steroid hormone receptors in human skin appendage and its neoplasms. *Endocr J* 2005; **52**: 317–25.

Molecular Genetics and Metabolism 99 (2010) 18–25

Contents lists available at ScienceDirect

Molecular Genetics and Metabolism

journal homepage: www.elsevier.com/locate/ymgme

Japan Elaprase® Treatment (JET) study: Idursulfase enzyme replacement therapy in adult patients with attenuated Hunter syndrome (Mucopolysaccharidosis II, MPS II)

Torayuki Okuyama [a,*], Akemi Tanaka [b], Yasuyuki Suzuki [c], Hiroyuki Ida [d], Toju Tanaka [e], Gerald F. Cox [f,g], Yoshikatsu Eto [h], Tadao Orii [i]

[a] Department of Clinical Laboratory Medicine, National Center for Child Health and Development, 2-10-1 Okura, Setagaya-ku, Tokyo 157-8535, Japan
[b] Department of Pediatrics, Osaka City University Graduate School of Medicine, Osaka, Japan
[c] Medical Education Development Center, Gifu University School of Medicine, Gifu, Japan
[d] Department of Pediatrics, The Jikei University School of Medicine, Tokyo, Japan
[e] Department of Clinical Genetics and Molecular Medicine, National Center for Child Health and Development, Tokyo, Japan
[f] Genzyme Corporation, Cambridge, MA, USA
[g] Division of Genetics, Children's Hospital Boston and Department of Pediatrics, Harvard Medical School, Boston, MA, USA
[h] Lysosomal Disease Research Center/Institute for Genetic Disease, The Jikei University School of Medicine, Tokyo, Japan
[i] Emeritus Professor, Gifu University, Gifu, Japan

ARTICLE INFO

Article history:
Received 25 June 2009
Received in revised form 20 August 2009
Accepted 20 August 2009
Available online 24 August 2009

Keywords:
Mucopolysaccharidosis II
Hunter syndrome
Clinical trial
Enzyme replacement therapy
Idursulfase
Elaprase

ABSTRACT

This open-label clinical study enrolled 10 adults with attenuated Mucopolysaccharidosis II and advanced disease under the direction of the Japan Society for Research on Mucopolysaccharidosis Disorders prior to regulatory approval of idursulfase in Japan. Ten male patients, ages 21–53 years, received weekly intravenous infusions of 0.5 mg/kg idursulfase for 12 months. Significant reductions in lysosomal storage and several clinical improvements were observed during the study (mean changes below). Urinary glycosaminoglycan excretion decreased rapidly within the first three months of treatment and normalized in all patients by study completion (−79.9%). Liver and spleen volumes also showed rapid reductions that were maintained in all patients through study completion (−33.2% and −31.0%, respectively). Improvements were noted in the 6-Minute Walk Test (54.5 m), percent predicted forced vital capacity (3.8 percentage points), left ventricular mass index (−12.4%) and several joint range of motions (8.1–19.0 degrees). Ejection fraction and cardiac valve disease were stable. The sleep study oxygen desaturation index increased by 3.9 events/h, but was stable in 89% (8/9) of patients. Idursulfase was generally well-tolerated. Infusion-related reactions occurred in 50% of patients and were mostly mild with transient skin reactions that did not require medical intervention. Two infusion-related reactions were assessed as serious (urticaria and vasovagal syncope). One patient died of causes unrelated to idursulfase. Anti-idursulfase antibodies developed in 60% (6/10) of patients. In summary, idursulfase treatment appears to be safe and effective in adult Japanese patients with attenuated MPS II. These results are comparable to those of prior studies that enrolled predominantly pediatric, Caucasian, and less ill patients. No new safety risks were identified.

Introduction

Mucopolysaccharidosis type II (MPS II, Hunter syndrome, OMIM #309900) is an X-linked recessive, lysosomal storage disorder caused by a deficiency of iduronate-2-sulfatase (IDS, EC3.1.6.13). This lysosomal enzyme catalyzes the first step in the degradation of the glycosaminoglycans (GAG), dermatan sulfate and heparan sulfate [1]. Iduronate-2-sulfatase deficiency leads to the accumulation of GAG within the lysosomes of virtually every cell in the body and is excreted in excessive amounts in the urine. MPS II encompasses a wide phenotypic spectrum that includes severe and attenuated forms. The severe form has onset of symptoms by 2–4 years old, progression of somatic symptoms and severe cognitive impairment during childhood, and death by 10–15 years of age. The attenuated form has a later onset in childhood, slower and milder progression of somatic disease, little to no cognitive impairment, and survival into adulthood. (Fig. 1) Common clinical features include coarse faces, upper airway obstruction, cardiac valve regurgitation, restrictive lung disease, hepatosplenomegaly, hernias, joint contractures, poor endurance, and reduced quality of life [2,3]. *IDS* gene mutations are heterogeneous, but some show genotype–phenotype correlations: deletions and gross rearrangements of the *IDS* gene are associated with the severe form, whereas missense

* Corresponding author. Fax: +81 3 3417 2238.
E-mail address: tora@nch.go.jp (T. Okuyama).

1096-7192/$ - see front matter © 2009 Elsevier Inc. All rights reserved.
doi:10.1016/j.ymgme.2009.08.006

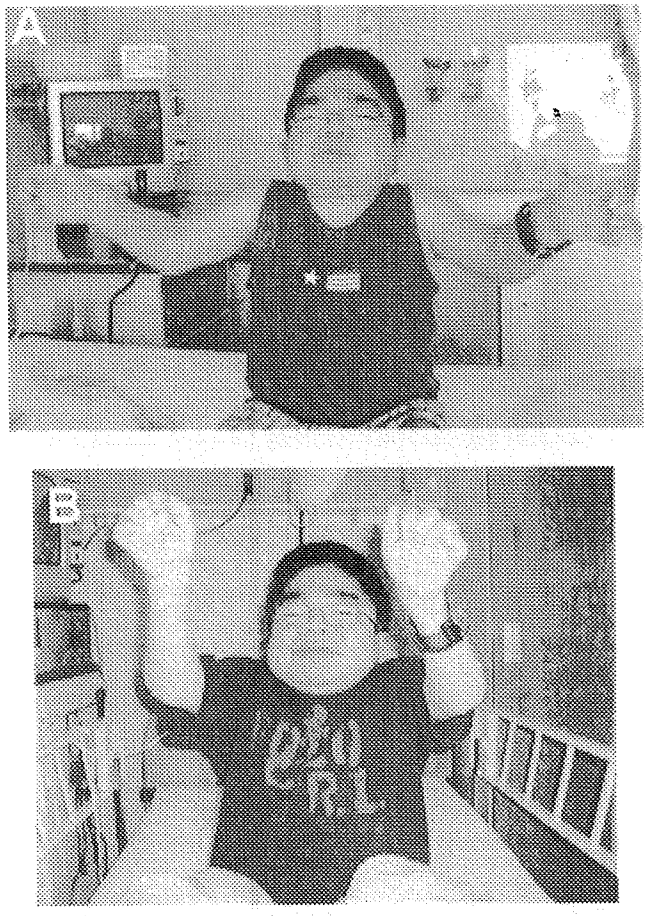

Fig. 1. A 23-year-old Japanese male study patient with MPS II. (A) Before treatment. (B) After 12 months of idursulfase treatment. Note the coarse facial features characteristic of MPS II. At baseline, the patient had severely limited shoulder range of motion (flexion and abduction), which improved following treatment.

mutations are more often associated with attenuated disease [4–10]. No racial or geographic differences have been observed. Females are only rarely affected, most often through skewed X-inactivation [1]. MPS II is the most prevalent MPS disorder in Asia, accounting for >50% of all MPS patients in Japan [10]. The annual incidence of all MPS disorders in Japan is estimated to be 1/50,000–1/60,000, and approximately half of the cases are due to MPS II. The estimated birth incidence of MPS II in Japan is, therefore, 1/90,000–1/100,000 [11], similar to the 1/92,000 to 1/162,000 incidences reported for predominantly Caucasian countries [12–15].

Until recently, treatment of MPS II was mainly palliative and focused on alleviating clinical symptoms through a variety of surgeries, medical devices, therapies, and medications. Several patients have undergone hematopoietic stem cell transplant (HSCT) as a source of iduronate-2-sulfatase, but unlike for MPS I, cognitive decline is not halted and the long-term effects on somatic disease are not well-documented [16,17]. Therefore, most centers consider the risk–benefit profile unfavorable and do not recommend HSCT for patients with MPS II.

Idursulfase (Elaprase®, Shire Human Genetic Therapies, Inc., Cambridge, MA, USA) is a recombinant human form of iduronate-2-sulfatase that is produced in a human cell line. Preclinical studies carried out in an MPS II knockout-mouse model [18] and in a Phase 1/2 dose-ranging study of MPS II patients [19] indicated that idursulfase was effective at reducing lysosomal GAG. The safety and efficacy of idursulfase was confirmed in a Phase 2/3 double-blind, placebo-controlled clinical study that randomized 96 MPS II patients to one of three treatment arms for 52 weeks: 0.5 mg/kg idursulfase weekly, 0.5 mg/kg idursulfase alternating with placebo every other week, or placebo weekly [20]. The primary efficacy endpoint was a composite of changes in percent predicted forced vital capacity (FVC) and the 6-Minute Walk Test (6MWT). Patients who received weekly idursulfase showed a greater difference in the composite endpoint compared to placebo ($p = 0.005$) than did the every other week idursulfase group ($p = 0.042$). The weekly idursulfase arm showed a mean 44.3 m increase in 6MWT distance (37 m difference from placebo, $p = 0.013$) and a mean 3.45 percentage point increase in percent predicted FVC (2.7 percentage point difference from placebo, $p = 0.065$). These clinical changes were associated with significant reductions versus placebo in urinary GAG level (−52.5%, $p < 0.0001$), liver volume (−25.3%, $p < 0.0001$), and spleen volume (−25.1%, $p < 0.0001$). Idursulfase was well-tolerated, with infusion-related reactions being the most common drug-related related adverse events, occurring in 69% (22/32) of patients in the weekly idursulfase arm.

Idursulfase was approved for the treatment of MPS II by the United States Food and Drug Administration (FDA) in July 2006 and by the European Medicines Agency (EMEA) in January 2007. Due to the life-threatening nature of the disease and the small number of patients, the Japanese Ministry of Health, Labour, and Welfare (MHLW) Committee for the Use of Unapproved Drugs recommended that idursulfase be approved based on ethical grounds and the results of overseas clinical trials, which included four Japanese patients. The committee also requested that idursulfase be made available to the most seriously ill MPS II patients prior to approval, which occurred in October 2007. Consequently, the Japan Elaprase Treatment (JET) study was initiated under the direction of the Japan Society for Research on MPS Disorders. Here, we present the results of this study.

Materials and methods

Patients

To be eligible for the study, patients had to meet all of the following inclusion criteria: (1) Documented deficiency of iduronate-2-sulfatase enzyme activity of <10% of the lower limit of normal with a normal enzyme activity level of one other sulfatase. (2) Male and above 20 years of age. (3) Clinically advanced disease status with <80% predicted FVC and New York Heart Association Class II–IV. (4) Capable of showing improved quality of life. (5) Able to complete study assessments.

Patient exclusion criteria included: (1) Previous bone marrow or cord blood transplant. (2) Known hypersensitivity to one of the components of idursulfase. (3) Previous treatment with idursulfase. (4) Unable to receive weekly infusions of idursulfase at the patient's local hospital. All patients provided signed informed consent prior to enrollment.

Study design

This was a multi-center, open-label study that enrolled 10 adult males with MPS II at 5 clinical sites in Japan. The study adhered to the guidelines set forth in the Declaration of Helsinki. Idursulfase was manufactured by Shire Human Genetic Therapies, Inc. and distributed by Genzyme Corporation (Cambridge, MA, USA). Genzyme Corporation performed all statistical analyses, and Genzyme Japan KK (Tokyo, Japan) provided data management support.

Idursulfase

Patients were administered 0.5 mg/kg idursulfase diluted in saline to a final volume of 100 cc intravenously over 3 h on a weekly

basis (±3 days) for up to 12 months. Infusions rates were ramped up over the first hour as described in the Phase 2/3 study [20]. Patients were monitored during each infusion and were discharged 1 h after completing the infusion, if clinically stable.

Efficacy assessments

Urinary GAG level was determined as the concentration of uronic acid normalized for creatinine (mg/g creatinine) and was measured using the carbazole reaction at a central laboratory (SRL Medisearch, Tokyo, Japan) or at Osaka City University Hospital. Liver and spleen volumes were quantitated by computerized tomography (CT), with the upper limits of normal being 2.5% and 0.2% of body weight, respectively. Percent predicted FVC and the 6MWT were performed according to American Thoracic Society guidelines [21,22]. Cardiac structure and function were evaluated by echocardiography (two-dimensional and M-mode). Left ventricular mass index (LVMI) was calculated as the left ventricular mass normalized for body surface area, with normal values defined as <131 g/m^2. Active joint range of motion was measured by goniometry, and included the shoulder (flexion, extension, and abduction), elbow (flexion and extension), hip (flexion and extension), and knee (flexion and extension). Left and right joint ranges of motion for each were averaged for each patient. The sleep study oxygen desaturation index (ODI) was assessed by pulse oximetry and defined as the number of desaturations (<89% oxygen saturation or ⩾4% decrease in oxygen saturation from baseline lasting ⩾10 s) per hour of sleep. A normal ODI was considered to be <5 events/h [23].

Safety assessments

Safety evaluation included continuous monitoring of adverse events and periodic clinical laboratory and physical examination evaluations. Adverse events were reported by severity (mild, moderate, severe, life-threatening) and by relatedness to idursulfase. An infusion-related reaction was defined as any adverse event occurring during or following an infusion (i.e., within 24 h of infusion initiation) that was reported by the investigator as related to idursulfase. Antibodies to idursulfase were measured by an enzyme-linked immunosorbant assay (ELISA; Shire Human Genetic Therapies).

Statistics

Efficacy results are reported as the mean ± standard error of the mean (SEM). For missing data at 12 months, the last observation carried forward method was used for values obtained at 6 months or later. The number of evaluable patients was at least nine for each endpoint, except for LVMI ($n = 6$, primarily due to missing baseline data) and the 6MWT ($n = 7$, primarily due to the inability to perform the test). The Wilcoxon signed rank test was used to evaluate changes in efficacy endpoint from baseline to 12 months, and p-values <0.05 were considered statistically significant. Percent change was tested for pharmacodynamic parameters (i.e., urinary GAG level and liver and spleen volumes), whereas absolute change was tested for clinical endpoints.

Results

Patient disposition

Ten adult Japanese males with attenuated MPS II were enrolled in the study and received idursulfase treatment. Nine patients completed the 12-month study; one patient died of causes unrelated to idursulfase after receiving 41 of 44 scheduled infusions (see Safety Section). Compliance with treatment was excellent, with all 10 patients receiving >93% of scheduled infusions; 80% (8/10) of patients did not miss a single scheduled infusion.

Patients

The mean patient age was 30.1 years (range 21.1–53.9). All patients had been diagnosed during mid-childhood or adolescence with MPS II (mean age 7.9 years), and all had advanced disease burden at the time of enrollment into the study. All patients had short stature (height <3rd percentile for Japanese adult males). Past medical history was significant for the following MPS II-related features (n = number of patients): valvular heart disease consisting mainly of aortic and/or mitral valve insufficiency (10), joint contractures (7), hepatomegaly (7), deafness (6), retinal degeneration (5), sleep apnea (5), otitis media

Table 1
Summary of efficacy changes after 12 months of treatment with idursulfase.

	N	Baseline	12 months	Change	% Change	p-Value
Urinary GAG (mg/g creatinine)	9	106.4 ± 7.8	21.2 ± 2.9	−85.2 ± 7.1	−79.9 ± 2.2	0.004†
Liver volume (cc)	10	1491.2 ± 92.9	993.2 ± 75.0	−498.0 ± 70.2	−33.2 ± 4.0	0.002†
Spleen volume (cc)	10	210.2 ± 22.5	138.1 ± 12.5	−72.1 ± 15.7	−31.0 ± 5.5	0.002†
6-Minute Walk Test (m)	7	286.0 ± 53.4	340.5 ± 49.6	54.5 ± 27.0	37.4 ± 18.1	0.109
Forced vital capacity (% predicted)	9	39.9 ± 6.6	43.7 ± 6.0	3.8 ± 2.8	15.0 ± 8.0	0.250
Forced vital capacity (L)	9	1.4 ± 0.3	1.5 ± 0.2	0.1 ± 0.1	16.3 ± 8.0	0.250
Left ventricular mass index (g/m^2)	6	139.9 ± 25.1	133.2 ± 38.9	−6.7 ± 15.5	−12.4 ± 11.1	0.563
Left ventricular ejection fraction (%)	10	67.0 ± 5.2	64.3 ± 6.0	−2.8 ± 2.5	−6.1 ± 5.7	0.244
Joint range of motion (degrees)					NA	
Shoulder flexion	10	93.8 ± 4.9	109.8 ± 7.1	15.0 ± 7.3		0.066
Shoulder extension	10	44.1 ± 4.1	43.8 ± 3.8	−0.3 ± 4.1		0.945
Shoulder abduction	10	76.3 ± 3.9	95.3 ± 8.1	19.0 ± 8.8		0.125
Knee flexion	9	103.7 ± 8.5	114.4 ± 5.2	10.7 ± 10.3		0.461
Knee extension	9	−11.1 ± 4.5	−10.3 ± 5.0	0.8 ± 2.5		0.875
Hip flexion	9	89.2 ± 8.1	103.3 ± 7.6	14.2 ± 5.1		0.031
Hip extension	9	3.1 ± 5.0	1.9 ± 6.7	−1.3 ± 1.8		0.750
Elbow flexion	10	120.9 ± 4.0	121.8 ± 3.7	0.9 ± 2.5		0.828
Elbow extension	10	−43.1 ± 4.2	−35.0 ± 4.2	8.1 ± 3.4		0.063
Oxygen desaturation index (events/h)	9	18.5 ± 6.1	22.3 ± 7.4	3.9 ± 3.5	NA	0.426

The last observation carried forward (LOCF) method was used to replace a missing value at the 12-month timepoint.
All values are the observed means ± SEM. All p-values are based on the Wilcoxon signed rank test for change from baseline to the 12-month timepoint.
NA, not applicable. Some patients had values of 0 at baseline that precluded calculation of percent change.
† The p-value is based on the Wilcoxon signed rank test for % change from baseline to the 12-month timepoint.

(4), macroglossia (3), umbilical hernia (2), carpal tunnel syndrome (2), heart failure (2), and left ventricular hypertrophy (1).

Urinary glycosaminoglycan (GAG)

All nine evaluable patients had elevated urinary GAG levels at baseline (mean 106.4 mg/g creatinine, approximately 8 times the upper limit of normal); one patient lacked an appropriate baseline value (Table 1). Following idursulfase treatment, urinary GAG levels decreased rapidly within the first three months of treatment and remained low for the remainder of the study (Fig. 2A). There was a statistically significant mean decrease in the urinary GAG level of −79.9 ± 2.2% from baseline to 12 months ($p = 0.004$). All nine evaluable patients showed a >70% decrease in urinary GAG levels and had normal values by the end of the study.

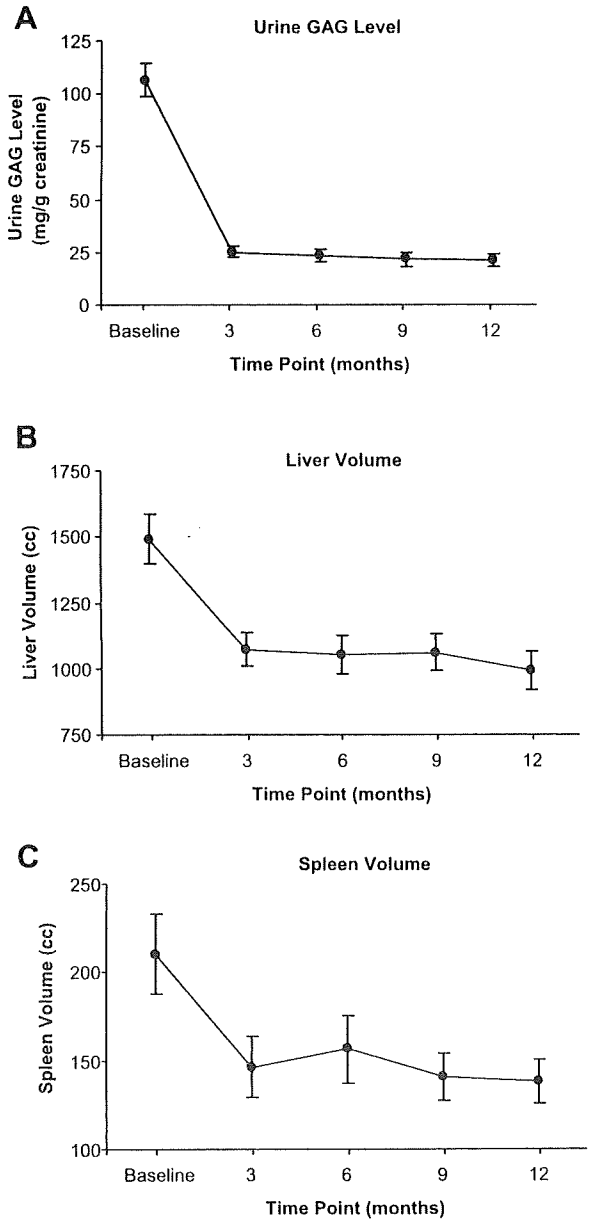

Fig. 2. The effects of idursulfase treatment on lysosomal storage over 12 months. (A) Urinary GAG level. (B) Liver volume. (C) Spleen volume. All changes are reported as mean ± SEM.

Liver and spleen volumes

At baseline, 9 (90%) patients had hepatomegaly (mean 1.3 MN, multiples of normal) and all 10 (100%) patients had splenomegaly (mean 2.4 MN) by CT. After 12 months of treatment, mean liver volume decreased by −33.2 ± 4.0% and mean spleen volume decreased by −31.0 ± 5.5% (Fig. 2B and C; Table 1), and both changes were statistically significant ($p = 0.002$). Most of the reductions occurred within the first three months of treatment. By the end of the study, all patients had liver volumes within the normal range and spleen volumes that were <2 MN, demonstrating efficient reduction of lysosomal GAG storage.

6-Minute Walk Test (6MWT)

At baseline, the mean 6MWT distance was 286.0 m for the seven patients who could perform the test (Table 1). All but one patient walked <399 m, the lower limit of normal for healthy adult men in the United States [24]. Three patients could not perform the 6MWT: one patient broke his leg just prior to the start of the study; one patient was wheelchair-bound secondary to shortness of breath and muscle weakness; and one patient was obese and could only walk a few steps with assistance. By the end of the study, the mean 6MWT distance had increased by 54.5 ± 27.0 m (Fig. 3A). This change represents a relative increase of 37.4%, and included one patient whose 6MWT distance increased by 131%. Four patients (57%) showed a clinically meaningful improvement of ⩾54 m [25], while the one patient with a normal 6MWT at baseline showed a decline (−71 m).

Percent predicted forced vital capacity (FVC)

Nine patients underwent spirometry at baseline and all showed a restrictive lung disease pattern: three were classified as having a severe defect (<50% predicted FVC) and five had a very severe defect (<34% predicted FVC) [26]. At baseline, mean percent predicted FVC was 39.9% (Table 1), and after 12 months it increased by 3.8 ± 2.8 percentage points (Fig. 3B). This improvement corresponds to a relative increase of 15.0% over baseline, which is considered clinically meaningful (⩾15% relative change) [25] and was achieved by four (44%) patients. Similarly, mean FVC increased by 16.3% over the baseline of 1.4 L. The mean forced expiratory volume in 1 s (FEV_1):FVC ratio remained unchanged at 0.70 during the study.

Cardiac

All patients had valve disease that remained stable during the study. The mean ejection fraction (EF) was normal at baseline and showed little change over 12 months (67.0–64.3%, change of −2.8 ± 2.5%) (Table 1). One patient with pre-existing cardiac failure showed gradual worsening during the study (EF 27–14%). At baseline, mean LVMI was slightly elevated at 139.9 g/m^2 (normal <131 g/m^2), and 50% (3/6) of evaluable patients had an elevated LVMI. After 12 months, mean LVMI decreased by −12.4%, with four patients showing a clinically meaningful improvement of >10% [27]. The patient with the largest LMVI at baseline showed a further increase (254.1–312.9 g/m^2).

Joint range of motion

Fig. 4 and Table 1 show the changes in joint range of motion observed during the study. At baseline, patients had significant joint contractures involving the shoulder (flexion, extension, and abduction), knee (flexion and extension), hip flexion and extension), and elbow (flexion and extension). Following 12 months of treatment, several joints showed increased range of motion, including mean

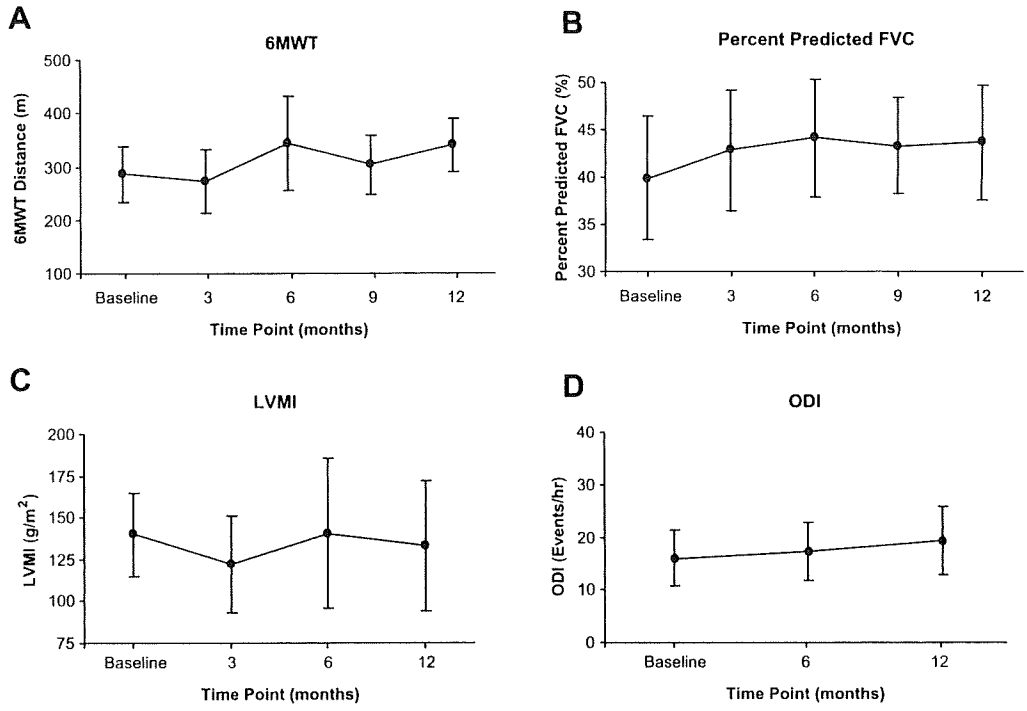

Fig. 3. The effects of idursulfase treatment on clinical endpoints over 12 months. (A) 6-Minute Walk Test. (B) % Predicted forced Vital Capacity. (C) Left Ventricular Mass Index. (D) Oxygen Desaturation Index. All changes are reported as mean ± SEM.

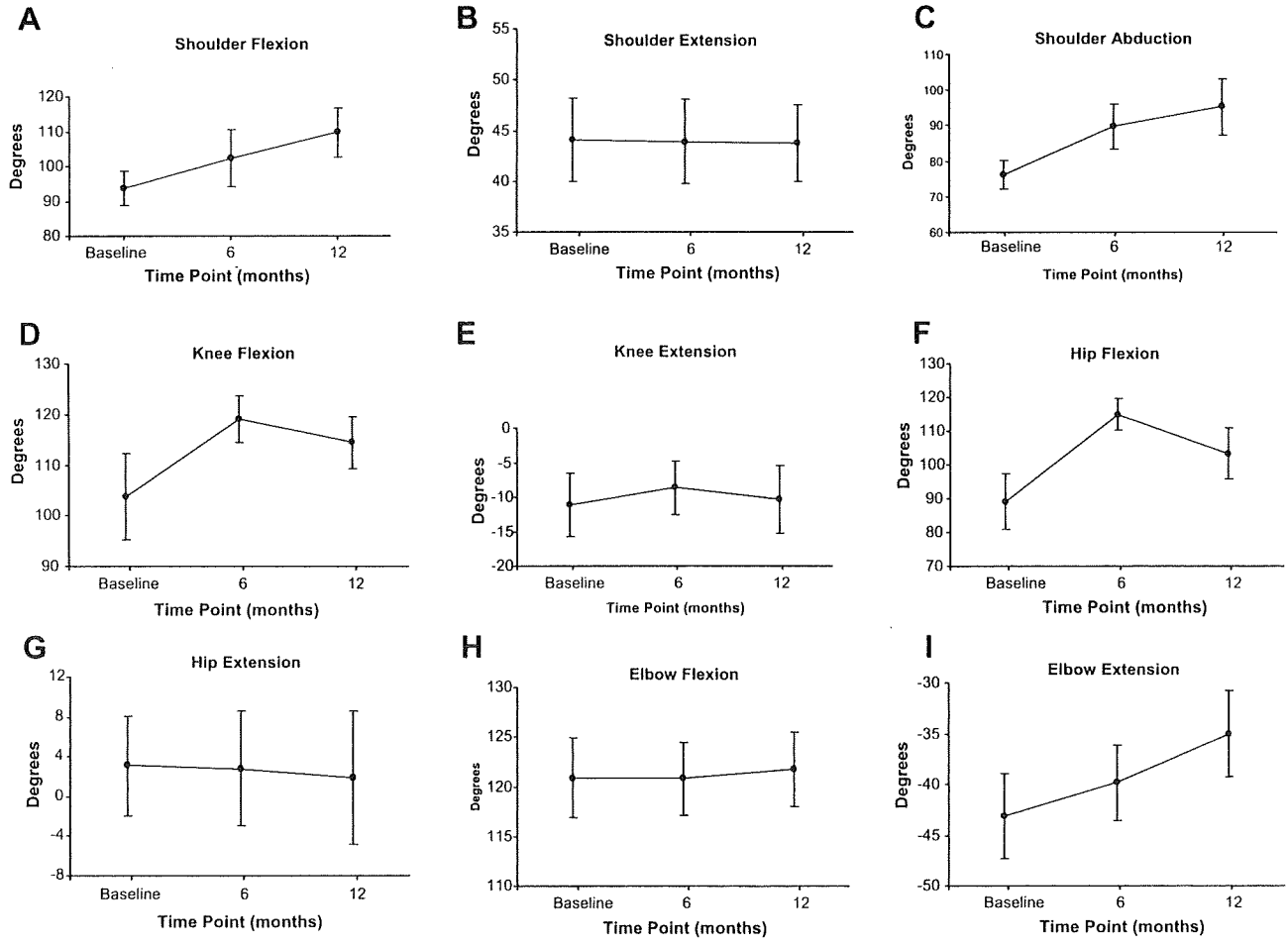

Fig. 4. The effects of idursulfase treatment on joint range of motion over 12 months. (A) Shoulder flexion. (B) Shoulder extension. (C) Shoulder abduction. (D) Knee flexion. (E) Knee extension. (F) Hip flexion. (G) Hip extension. (H) Elbow flexion. (I) Elbow extension. All changes are reported as mean ± SEM.

shoulder flexion (15.0 ± 7.3 degrees), shoulder abduction (19.0 ± 8.8 degrees), knee flexion (10.7 ± 10.3 degrees), hip flexion (14.2 ± 5.1 degrees; $p = 0.031$), and elbow extension (8.1 ± 3.4 degrees). However, most of the changes did not achieve statistical significance. Shoulder extension (−0.3 ± 4.1 degrees), elbow flexion (0.9 ± 2.5 degrees), knee extension (0.8 ± 2.5 degrees), and hip extension (−1.3 ± 1.8 degrees) showed little change during the study. Fig. 1 shows a 23 year-old study patient with severely limited shoulder range of motion (abduction and flexion), which improved following one year treatment with idursulfase.

Oxygen desaturation index (ODI)

At baseline, the mean oxygen desaturation index (ODI) was 18.5 events/h ($n = 9$), which is moderately abnormal [23]. Three patients had a normal ODI (<5 events/h), two had a mildly abnormal ODI (5–15 events/h), and four had a moderately to severely abnormal ODI (>15 events/h). During the study, the mean ODI increased by 3.9 ± 3.5 events/h, which was largely due to a single patient with an increase of 26.8 events/h. The other seven patients had stable ODI values (changes ⩽ 10 events/h).

Safety

Idursulfase was well-tolerated over the course of the study. Adverse events were mainly mild, unrelated, and attributable to expected symptoms of MPS II disease. Fifty percent (5/10) of patients experienced a total of 11 drug-related adverse events. Urticaria was the most frequent event (five events in two patients), followed by erythema (two events in the same patient). Similarly, 50% (5/10) of patients experienced infusion-related reactions (i.e. adverse events assessed as drug-related and occurring within 24 h of the infusion). The highest patient incidence involved skin reactions, i.e. urticaria and erythema (three patients each), while dyspnea, abdominal pain, and vasovagal syncope also were observed in one patient each. Except for one patient who experienced several episodes of urticaria between 9 and 12 months, the other four patients had infusion-related reactions only once or twice during the first three months of treatment. Management of infusion-related reactions included antihistamine therapy and temporary interruption of the infusion, and all events were followed by a successful patient recovery. There were no clinical laboratory abnormalities reported as related to idursulfase.

Two patients experienced serious adverse events, including one death, in the study. A 26 year-old male experienced an infusion-related reaction involving diffuse urticaria, flushing, and numbness of the tongue 1 h after initiation of the fifth infusion. The patient was pre-medicated with antihistamines without further events. A 42 year-old male had an infusion-related reaction reported by the investigator as vasovagal syncope, which consisted of hypotension, vomiting, weak pulse, and decreased consciousness and occurred 30 min into the first infusion. Subsequent infusions were preceded by corticosteroid pre-medication administration without further infusion-related reactions. The patient had a history of cardiac valve incompetence and cardiac failure requiring medications, including furosemide. Later in the study, he experienced an increase in leg edema secondary to worsening congestive heart failure. He was depressed and attempted suicide by drug overdose (not idursulfase). Upon arrival at the hospital, the patient went into cardiac arrest. Subsequent resuscitation measures were unsuccessful, and he died due to hypoxic encephalopathy, pneumonia and renal failure.

Antibodies

Anti-idursulfase IgG antibodies were detected in 60% (6/10) of patients, two of who became seronegative later in the study. No IgE antibodies were detected in patients who underwent testing for infusion-related reactions. The mean reductions in urinary GAG levels did not differ between patients who were seropositive at any time (−80.9% ± 3.8%; $n = 5$) and those who remained seronegative throughout the study (−78.6% ± 1.8%; $n = 4$). Although hypersensitive reactions or infusion-related adverse reactions tended to occur in the antibody-positive patients (four antibody-positive patients versus one antibody-negative patient), there was no correlation between the presence of antibodies and other adverse events. Furthermore, the frequency of hypersensitivity reactions did not correlate with antibody titer.

Discussion

The most remarkable difference between this and previous clinical studies of idursulfase [19,20] relates to the patient demographics and characteristics. The purpose of the JET study was to provide access to treatment for the most seriously ill MPS II patients while awaiting regulatory approval of idursulfase in Japan, which occurred in October 2007. Patients in the JET study had a mean age of 30.1 years, all were Japanese, and all were seriously ill (mean percent predicted FVC 39.9% and mean 6MWT distance 286.0 m). By comparison, MPS II patients in the Phase 1/2 and Phase 2/3 studies of idursulfase were younger (mean ages 13.9 years and 14.2 years), predominantly Caucasian (100% and 83%, respectively), and less severely affected (mean percent predicted FVC 55.1% and 55.4%; mean 6MWT distance 397 m and 395 m) [19,20]. Despite these patient differences, the JET study has shown that idursulfase is a safe and effective (Table 1) treatment for Japanese patients with MPS II and its risk–benefit profile is similar to that reported in previous studies.

In this study, idursulfase efficiently reduced GAG storage, as evidenced by the statistically significant reductions in urinary GAG levels ($p = 0.004$) and hepatosplenomegaly ($p = 0.002$) (Fig. 2; Table 1). These pharmacodynamic changes appeared to translate into clinical benefit, as evidenced by trends towards improvement in functional capacity (mean 54.5 m increase in 6MWT), respiratory function (mean 15.0% relative increase in percent predicted FVC), joint range of motion (mean increases ranging from 8.1–19.0 degrees for several joints), and LVMI (mean −12.4% decrease). Cardiac EF and valve disease remained mostly stable, although one patient with severe congestive heart failure showed progressive worsening and one patient with a greatly elevated LVMI showed a further increase. The mean ODI increased slightly by 3.9 events/h, but importantly 89% (8/9) of patients showed no clinically significant changes.

The safety profile of idursulfase in the JET study was similar to that of previous studies with no new or unexpected adverse events despite the older and more seriously ill patient population. Most adverse events were considered by investigators to be disease-related and unrelated to idursulfase. The most common drug-related adverse events were infusion-related reactions, occurring in 50% of patients. The most common infusion-related reactions were skin reactions consisting of urticaria and erythema. There were two related serious adverse events that occurred during the infusions—one involving urticaria, flushing, and numbness of the tongue, and the other involving vasovagal syncope. The one patient death was attributed to suicide from a drug overdose and was not related to idursulfase.

MPS II is a progressive and debilitating multisystem disease that is associated with a shortened lifespan, primarily from cardiorespiratory compromise [28]. Therefore, it is noteworthy that in this one-year study, cardiac and respiratory functions were improved or stable in most patients. Decreasing lung volumes are known to be associated with increased morbidity and mortality [26];